# NATIONAL ADVISORY COMMITTEE FOR AERONAUTICS

TECHNICAL NOTE

No. 1366

# EFFECT OF CHANGING MANIFOLD PRESSURE, EXHAUST PRESSURE, AND VALVE TIMING ON THE AIR CAPACITY AND OUTPUT OF A FOUR-STROKE ENGINE OPERATED WITH INLET VALVES OF VARIOUS DIAMETERS AND LIFTS

By James C. Livengood and James V. D. Eppes
Massachusetts Institute of Technology

Washington
December 1947

NATIONAL ADVISORY COMMITTEE FOR AERONAUTICS

TECHNICAL NOTE NO. 1366

# EFFECT OF CHANGING MANIFOLD PRESSURE, EXHAUST PRESSURE, AND VALVE TIMING ON THE AIR CAPACITY AND OUTPUT OF A FOUR-STROKE ENGINE OPERATED WITH INLET VALVES OF VARIOUS DIAMETERS AND LIFTS

By James C. Livengood and James V. D. Eppes

## SUMMARY

A series of tests has been made with a CFR engine to determine the effect of inlet-valve capacity, inlet and exhaust pressure, and valve timing on the volumetric efficiency at various speeds. Three combinations of inlet and exhaust pressures and seven valve-timing arrangements were used. Special cylinder heads with different sizes of inlet valves were provided. The engine was tested with the inlet valves operated at different lifts.

It was found that when the engine was operated with any one of the combinations of inlet pressure, exhaust pressure, and valve timing, the variation of volumetric efficiency resulting from changes in inlet-valve size and lift could be expressed as a function of the parameter $\phi$, defined as follows:

$$\phi = \frac{\text{piston speed} \times \text{piston area}}{\text{sound velocity} \times \text{inlet-valve area} \times \text{average flow coefficient}}$$

provided other design ratios and operating conditions were kept constant. The average flow coefficient was determined from steady-flow tests of the inlet valve and port and from the diagram of valve opening against crank angle. The inlet-valve area was taken as the area of a circle the diameter of which was equal to the minimum diameter of contact between valve and seat. Sound velocity was computed for air at inlet-mixture temperature.

Closing the inlet valve late resulted in improved volumetric efficiency when the engine was operated at high values of $\phi$ and reduced volumetric efficiency at low values of this parameter.

Increasing the amount of valve overlap improved the volumetric efficiency when the engine was operated with $\frac{\text{exhaust pressure}}{\text{inlet pressure}} \gtrsim 1$. This effect increased with decreasing values of $\phi$.

Variations of volumetric efficiency resulting from changes in inlet and exhaust pressure were found to be functions of more than inlet and exhaust pressure.

## INTRODUCTION

In reference 1 the variables that affect the volumetric efficiency of an internal-combustion engine were classified into two categories:

1. Operating conditions, such as revolutions per minute, inlet and exhaust pressures, operating temperatures, and so forth.

2. Design factors, including design of cylinder, valves, inlet and exhaust manifolds, valve timing, and so forth.

The investigation reported in reference 1 showed that for the particular inlet and exhaust pressures, valve timing, and temperatures used, the effect of inlet-valve diameter, lift, and design on the volumetric efficiency of an engine operated over a speed range could be summed up in the following expression[1]:

$$e = f(\phi)$$

The factor $C_{av}$ was determined from steady-flow tests and the inlet-valve lift against crank-angle relationships. The method of determination is described in reference 1 and is reproduced in appendix A for convenience.

While the investigation of reference 1 showed good correlation of results within the range of variables covered, it seemed desirable to extend the range of revolutions per minute to very low values and to investigate the effects of inlet and exhaust pressures and of valve timing upon the correlation.

The objects of the tests reported herewith were:

1. To test the validity of the conclusions of reference 1 at inlet pressures and exhaust pressures other than those used in that work.

---

[1]The symbols and definitions of terms used in this report appear in appendix B.

2. To investigate the possibility of correlating the relationships between volumetric efficiency and inlet and exhaust pressures.

3. To determine the effect on volumetric efficiency of changing the crank angle at which the inlet valve closed.

4. To determine the effect on volumetric efficiency of changing valve overlap.

The tests were made at the Sloan Laboratories of the Massachusetts Institute of Technology under the sponsorship and with the financial assistance of the National Advisory Committee for Aeronautics.

## DESCRIPTION OF APPARATUS

### Engine

A CFR single-cylinder engine of 3.25-inch bore and 4.5-inch stroke was used. This engine was the same as that described in reference 1 except that a special cylinder was used which did not require the use of an aluminum spacer between cylinder and cylinder head. This engine was connected to an electric cradle dynamometer, the setup being conventional except as noted in the following discussion.

### Inlet System

Air supplied to the engine was taken from the laboratory compressed air line and passed successively through a sharp-edge orifice installed in a pipe in accordance with the specifications of reference 2, a pulsation damper consisting of two 20-gallon tanks connected in series through a restriction, a throttle valve for controlling inlet pressure, a heated vaporizing tank, and a large, short intake pipe leading to the engine.

The fuel, exhaust, cooling, and lubrications systems remained the same as described in reference 1.

### Camshafts

The camshafts were of the same general design as the one used in reference 1. One of these, Camshaft 2 in figure 1, was the camshaft used in reference 1. The remaining six camshafts shown in figure 1 had different timings. When a given cam had a longer or shorter duration than the cams of Shaft 2, its profile was developed by expanding or

contracting each angular increment of the curve of lift against cam angle, according to the total duration of valve opening required. Note that there is one series of three camshafts with 60° overlap and variable inlet closing angle, another series with substantially no overlap and variable inlet closing angle, and a third series in which the inlet valve closes at 60° A.B.C., and the exhaust valve opens at 60° B.B.C., but with overlaps of 90°, 60°, and 6°. The actual cam lift was constant in all cases, and valve lift was varied by means of rocker-arm adjustments as explained in reference 1.

## Valves

The valves used were the large ($D_V$ = 1.05 in.) and small ($D_V$ = 0.830 in.) inlet valves of the geometrically similar series in reference 1. The exhaust valve was standard CFR exhaust valve, which is larger than the large inlet valve. The two inlet valves had identical flow coefficients at a given lift-diameter ratio. The method of determining these steady-flow coefficients is described in appendix A.

## Measuring Instruments

All measurements were made in the manner described in reference 1 except that torque was measured by a hydraulically balanced piston and mercury manometer, instead of by beam scales, and air was measured by a sharp-edge orifice installed in a pipe instead of on an air box. Pressure drop across the orifice was measured with an NACA micromanometer filled with distilled water.

Indicated horsepower was calculated from indicator diagrams made with the M.I.T. balanced-diaphragm high-speed indicator.

# PROCEDURE

The air capacity of the engine was carefully measured over a speed range from 500 to 3600 rpm, with the exception of tests made with Camshafts 4, 5, and 6, which were run only to 3200 rpm because of exhaust-valve jumping resulting from the short exhaust duration of these cams. Fuel-air ratio was held constant, and spark advance was adjusted to best power for each condition. The following table shows which engine conditions were held constant and which were varied, and the specific values or range of values are indicated.

Engine quantities that were held constant:

| | |
|---|---|
| Inlet-mixture temperature, °F | 120 |
| Fuel-air ratio | 0.078 |
| Oil temperature, °F | 160 |
| Jacket-water-outlet temperature, °F | 180 |
| Inlet-valve running clearance, in | 0.010 |
| Exhaust-valve running clearance, in | 0.010 |
| Compression ratio | 4.9 |

Engine quantities that were varied:

| | |
|---|---|
| Engine speed, rpm | 500 to 3600 |
| Inlet-valve and lower-inlet-port diameter, in | 1.050 and 0.830 |
| Inlet-valve lift, in | 0.262 and 0.208 |
| Inlet pressure, in. Hg abs | 30 and 40 |
| Exhaust pressure, in. Hg abs | 30, 20, and 10 |
| Spark advance | Always best power |
| Inlet- and exhaust-valve timing | See timing diagrams in fig. 1. |

## TESTS

With each of the seven camshafts shown in figure 1, a series of nine runs was made. This series consisted of three runs with each of the following arrangements of inlet-valve diameter and lift:

| $D_v$ (in.) | L (in.) |
|---|---|
| 1.05 | 0.262 |
| 1.05 | .208 |
| .830 | .208 |

With each diameter-lift-cam combination, runs of eight or nine points each over a speed range were made with each of the following inlet- and exhaust-pressure combinations:

| $p_i$ (in. Hg abs.) | $p_e$ (in. Hg abs.) |
|---|---|
| 30 | 30 |
| 40 | 20 |
| 40 | 10 |

## DISCUSSION OF RESULTS

Data obtained with Camshaft 1 are presented in table I, which lists the speed, air flow, volumetric efficiency, brake and indicated horsepower, and $\phi$ for the tests. The various graphs discussed in this section are derived from this data and similar data obtained with the other camshafts.

Figures 2 to 22 show that for any particular valve timing and inlet- and exhaust-pressure combination, volumetric efficiency e is a function of $\phi$, where

$$\phi = \left[ \frac{s}{c} \left( \frac{D_p}{D_v} \right)^2 \frac{1}{C_{av}} \right]$$

over a wide range of values of this parameter. This range of values was obtained by changing s, $D_v$, and valve lift. Both $D_v$ and valve lift affect $C_{av}$.

Over a large range of change in valve timing and inlet and exhaust pressure, the volumetric efficiency remains a function of the parameter $\phi$, although a different function for each timing and pressure combination. One underlying reason for these correlations would seem to be that the inlet valves used for these tests have substantially similar curves of flow coefficient against crank angle (fig. 23). These curves being similar, the ratio of the average flow coefficient $C_{av}$ (proportional to the area under each curve of fig. 23) to the flow coefficient at a given lift $C_l$ is constant at any particular crank angle. It should be pointed out that if the engine had been operated with inlet-valve lifts which resulted in greatly dissimilar curves of $C_l$ against crank angle, the correlations in figures 2 to 22 might have been less successful.

Figures 24 to 30 utilize the curves which were drawn through the points of figures 2 to 22. Each figure demonstrates the effect on volumetric efficiency of changing inlet and exhaust pressures with a particular valve-timing arrangement. An interesting feature of these curves is the rise in volumetric efficiency at low values of $\phi$. This rise is especially noticeable in the cases of figures 24, 25, 26, and 30, which were obtained with considerable valve overlap.

When there is high inlet pressure and low exhaust pressure, some of the fresh charge is blown through the cylinder and out the exhaust port. Presumably, the amount blown through per unit time is substantially independent of engine speed. Therefore, if the engine were run at extremely

low speed, the quantity of charge passing through the cylinder during the overlap period would be a large portion of the total flow, and the volumetric efficiency would approach infinity when the speed reached zero.

Some rise in volumetric efficiency at low speed is noted even for operation with inlet pressure equal to exhaust pressure. This rise is probably due to the ejector effect of the exhaust gases. The inertia of the rapidly moving exhaust gas at the end of blow-down may cause a low pressure of the residual exhaust gas and a consequent influx of fresh charge during the overlap period. Such an improvement in scavenging will result in increased volumetric efficiency, and the improvement would increase with decreasing speed, as indicated by the curves in question. A small amount of exhaust back pressure would overcome this effect, and volumetric efficiency would then remain constant at low speed or even decrease if the back pressure were large enough to produce reverse flow during the overlap period. This sensitivity to inlet and exhaust pressures at low speeds when $p_e/p_i = 1$ was so pronounced in the case of Camshaft 7 ($90^\circ$ overlap) that it was impossible to control the pressures with sufficient accuracy to permit precise volumetric-efficiency measurements below $\phi = 0.45$. Consequently, the results of such measurements are not plotted.

In an attempt to obtain a theoretical explanation for the effects of inlet and exhaust pressures on volumetric efficiency, the following simple analysis, suggested by Professor E. S. Taylor, was used:

A "square" pumping loop for an ideal air cycle is assumed as shown in figure 31. A thermodynamic "system" is chosen which consists of all the charge that will eventually be found in the cylinder at the start of compression. As the initial condition, the end of the exhaust stroke is chosen. The exhaust valve is assumed to be closed at this point, and the pressure in the cylinder is assumed to be exhaust pressure. The end of the suction stroke is taken as the final condition and the inlet valve is assumed to be closed at this point. If it is assumed that the pressure in the cylinder during the entire piston stroke is equal to the inlet pressure, the first law of thermodynamics for the inlet process can be written as follows:

$$J(M_r + M_i)E_1 - JM_rE_r - JM_iE_i = p_iV_i - p_i\left(V_1 - \frac{V_1}{r}\right) \qquad (1)$$

According to the relations for a perfect gas,

$$pV = \frac{M}{m}RT$$

Since $R = Jm(C_p - C_v)$ and $E = C_vT$,

$$JME = \frac{pV}{k - 1}$$

If this value is substituted in equation (1), the following result is obtained:

$$\frac{p_iV_i}{k-1} - \frac{p_e\left(\frac{V_1}{r}\right)}{k-1} - \frac{p_iV_i}{k-1} = p_iV_i - p_i\left(V_1 - \frac{V_1}{r}\right)$$

and

$$\frac{V_i}{V_1 - \frac{V_1}{r}} = 1 - \frac{\left(\frac{p_e}{p_i}\right) - 1}{k(r-1)}$$

The ratio of the volume of fresh air at inlet condition $V_1$ to the displacement volume $V_1 - \frac{V_1}{r}$ of the cylinder is called volumetric efficiency.

Thus

$$e_{ideal} = 1 - \frac{\left(\frac{p_e}{p_i}\right) - 1}{k(r-1)}$$

where $e_{ideal}$ is the volumetric efficiency for the ideal air cycle. It will be noted that this expression makes no attempt to account for the effects of valve overlap.

The foregoing analysis may be compared with that given on pages 234–235 of reference 3. (See also equation (52), page 246, reference 3.) It will be observed that the present analysis involves simpler assumptions and gives a simpler result. If $1.5 > p_e/p_i > 0.5$, the foregoing equation gives substantially the same result as equation (52) in reference 3. If $1.5 < p_e/p_i < 0.5$, the equation gives a slightly smaller correction than equation (52) reference 3.

A quantity called the adjusted volumetric efficiency is obtained by dividing the actual volumetric efficiency obtained from a test by the

corresponding ideal volumetric efficiency; that is, adjusted volumetric efficiency = $e/e_{ideal}$. Figures 32 to 38 show the result of applying this procedure to the curves of figures 24 to 30. The curves for operation with inlet pressure equal to exhaust pressure are unchanged, since $e_{ideal} = 1$; but the ordinates of the curves for operation with values of $p_e/p_i < 1$ are decreased. In the cases in which there was no valve overlap (figs. 35 to 37), this correction is more successful at low speeds than at high speeds. At high speeds, the curves are overcorrected. This overcorrection occurs because at high values of $\phi$ the actual pumping loop departs seriously from the square loop assumed in the analysis.

Figures 32, 33, 34, and 38 show results of operating with valve overlap. In these cases, adjusted volumetric efficiency gives a fairly good correction at high values of $\phi$ because the effect of scavenging of the clearance space during the overlap period approximately offsets the effect of the departure of the pumping loop from the square form. The success of the correction appears, therefore, to be fortuitous. At low values of $\phi$ the pumping loop is more nearly square, but the effect of scavenging during the overlap period is much larger. The correction is therefore too small.

Figures 39 and 40 show the effect of varying the inlet-valve closing angle on the volumetric efficiency of the engine. Curves are drawn for three values of $\phi$, as well as for three inlet- and exhaust-pressure combinations. At low values of $\phi$ (low gas velocities), late inlet-valve closing reduces volumetric efficiency because part of the fresh charge is pushed back into the inlet port by the rising piston. At high values of $\phi$, however, volumetric efficiency is improved by late inlet closing because the pressure in the cylinder remains lower than $p_i$ for a considerable time after bottom dead center. This lowered cylinder pressure is due to the high pressure drop across the inlet valve accompanying high values of $\phi$. These trends are not affected by inlet or exhaust pressures or by valve overlap.

Figure 41 is a photograph of a three-dimensional model illustrating the relationships between volumetric efficiency, the parameter $\phi$, and the crank angle at which the inlet valve closes. The lines which appear on the upper surface are contours of constant volumetric efficiency. This particular model shows the relationships with $p_e = p_i = 30$ inches of mercury absolute for camshafts with 60° overlap. However, the general character of the surface is not changed by overlap or inlet and exhaust pressures, as can be deduced from figures 39 and 40.

Figure 42 shows the indicated horsepower computed from indicator diagrams plotted against air flow for all combinations of $p_i$, valve size and lift, and valve timing. The plotted points include results obtained at

three different speeds for each combination, namely 500, 2000, and either 3200 or 3600 rpm. The group of points near the origin are all for 500 rpm. The points corresponding to the other speeds are not segregated.

Figure 42 shows that at 500 rpm the indicated specific air consumption is relatively high for all camshafts, perhaps because of high relative heat losses. At the higher speeds the specific air consumption obtained with Camshaft 7 (90° overlap) is high in nearly all instances, and the points obtained with Camshaft 3 are likewise high. The increased specific air consumption when the engine is operated with large overlap is probably due to loss of fresh charge during the overlap period. The reason for the increase in specific air consumption during operation with Camshaft 3 is not clear.

## CONCLUSIONS

An investigation was made at the Massachusetts Institute of Technology with a CFR engine to determine the effect of inlet-valve capacity, inlet and exhaust pressure, and valve timing on the volumetric efficiency at various speeds. Results from these tests indicated that:

1. The variation of volumetric efficiency resulting from changes in inlet-valve size and lift can be expressed as a function of the parameter $\phi$, defined as follows:

$$\phi = \frac{\text{piston speed} \times \text{piston area}}{\text{sound velocity} \times \text{inlet-valve area} \times \text{average flow coefficient}}$$

This is true for each of the 21 combinations of inlet pressure, exhaust pressure, and valve timing which were investigated.

2. The variation of volumetric efficiency resulting from changes in inlet and exhaust pressures cannot be expressed as a function of exhaust pressure $p_e$ and inlet pressure $p_i$ alone, but depends also upon other variables, including $\phi$ and probably the shape of the curve of valve flow coefficients against crank angle.

3. Closing the inlet valve late resulted in improved volumetric efficiency at high values of $\phi$ and reduced volumetric efficiency at low values of this parameter. This effect was the same for the three inlet- and exhaust-pressure combinations tested, and changing the valve overlap did not alter this trend.

4. Increasing the valve overlap resulted in improved volumetric efficiency when the engine was operated at values of $p_e/p_i \leq 1$. The effect was more marked at low values of $\phi$.

5. Indicated specific air consumption was very nearly constant over most of the upper range for all the tests except those in which the engine was operated with 90° A.B.C. inlet-valve closing and 60° valve overlap, or with 60° inlet-valve closing and 90° overlap. For these tests the indicated specific air consumption was somewhat higher.

6. Indicated specific air consumption was high at 500 rpm in all tests, even those without overlap.

Massachusetts Institute of Technology
Cambridge, Mass., May 4, 1945.

# APPENDIX A

## METHODS OF DETERMINING FLOW COEFFICIENTS FOR STEADY FLOW[1]

### The Flow Coefficient

The steady-flow coefficient for poppet valves as defined herewith has been developed to serve as a basis upon which to compare various valve and port combinations (references 4 to 7). The flow coefficient is an inverse measure of the resistance to flow through the valve and port at a given lift.

In determining the flow coefficient, a constant pressure drop is created across the valve and the rate of mass flow measured. For the low pressure drop usually used (10 in. alcohol), the flow coefficient is determined from the equation:

$$M_a = A_v C_l \sqrt{2\rho_v \Delta p_v}$$

in which the flow coefficient $C_l$ at a given lift is the only unknown.

The flow coefficient is based upon the nominal valve area $\frac{\pi}{4} D_v^2$. Changes in the actual area of the valve opening as the valve is lifted are reflected in the flow coefficient.

In order to make possible the comparison of valves of different diameter, it is necessary to compare the flow coefficients on the basis of a nondimensional parameter, in this case $L/D_v$. For valves of varying diameter but geometrically similar design, the flow coefficient is the same for a given value of $L/D_v$. In the steady-flow tests made for the present report a series of lifts was selected for each valve so that the flow coefficient was determined at intervals of $0.05\ L/D_v$ from 0 to 0.35. Figure 43 shows the apparatus used.

The selection of the diameter upon which the valve area and the $L/D_v$ ratio are based is optional. In this case the minimum contact diameter between valve and seat $D_v$ was used. Any other characteristic dimension could be used in place of $D_v$, for example, the outside diameter of the valve. When different valves are compared, however, it is necessary to use the same characteristic diameter.

---

[1]Adapted from reference 1. Some of the symbols, together with the reference numbers, have been changed to conform with the present report.

The flow coefficient of the valve at a given $L/D_v$ is calculated from the measurement made with the previously described apparatus by the following convenient formula, developed in reference 7 by equating the air flow through the metering orifice to the air flow through the valve:

$$M_a = A_o C_o \sqrt{2\rho_o \Delta p_o} = A_v C_l \sqrt{2\rho_v \Delta P_v}$$

and

$$C_l = \frac{A_o C_o}{A_v} \sqrt{\frac{\Delta p_o}{\Delta p_v}}$$

provided $\rho_o \cong \rho_v$, which is equivalent to having $\Delta p_o \ll p_o$.

## Intermittent Flow

The curve of $C_l$ against $L/D_v$ calculated by the method just described is obtained under steady-flow conditions. In the internal-combustion engine the flow is intermittent. The application of steady-flow results to intermittent conditions was at first questioned (reference 4), but the validity of its use was later established by Waldron (reference 6); Waldron's tests, however, were run at a speed range of 130 to 1200 rpm. The validity of the application of the steady-flow coefficients to intermittent conditions at the highest crank speeds used here has not been established. The success of the correlation of the engine test data indicates, however, that the steady-flow coefficient is very useful, whether or not it is an accurate measure of the coefficient in actual intermittent flow.

## The Average Flow Coefficient

The average flow coefficient used in the correlation of data is defined as:

$$C_{av} = \frac{1}{\theta_o} \int_o^{\theta_o} C_l \, d\theta$$

where $\theta_o$ is the number of crank degrees during which the valve is open, and $C_l$ is the flow coefficient corresponding to a given lift.

The average flow coefficient was determined in the following manner: First, the valve-lift curve was obtained from the cam profile and the rocker-arm ratio. From the curve of flow coefficient against lift-diameter ratio it was then possible to plot a curve of $C_l$ against $\theta$ (fig. 23).

The area under this curve was then measured with a planimeter, and the average flow coefficient $C_{av}$ was obtained by dividing this area by the length of the abscissa $\theta_o$ and multiplying by a scale factor.

## APPENDIX B

$A$ area

$c$ velocity of sound in inlet air

$C_{av}$ average flow coefficient of inlet valve (See appendix A.)

$C_l$ flow coefficient of inlet valve at a given lift (See appendix A.)

$C_o$ reference orifice coefficient in flow test (See appendix A.)

$C_p$ specific heat at constant pressure

$C_v$ specific heat at constant volume

$D_p$ O.D. of piston

$D_v$ diameter of minimum contact between inlet valve and seat

$e$ volumetric efficiency $\left( \frac{M_a}{\frac{N}{2} V_d \rho_i} \right)$

$e_{ideal}$ volumetric efficiency of ideal air cycle

$E$ internal energy per unit mass

$f$ function of terms in brackets

$J$ mechanical equivalent of heat

$k$ adiabatic compression exponent $\left(\frac{C_p}{C_v}\right)$

$L$ inlet-valve lift

$m$ molecular weight (29 for air)

$M$ mass

$M_a$ time rate of air flow, mass/unit time

$N$ rotational speed of crankshaft

$p$ pressure

$r$ compression ratio

$R$ universal gas constant

$s = 2 \times \text{stroke} \times N$, average piston speed

$T$ absolute temperature

$V$ volume

$V_d$ cylinder displacement volume

$\rho$ density

$\phi = \frac{s}{c}\left(\frac{D_p}{D_v}\right)^2 \frac{1}{C_{av}}$

$\theta$ crank angle, deg

$\theta_o$ crank angle during which valve is open, deg

Subscripts:

1 beginning of compression for ideal air cycle (See fig. 31.)

e exhaust pipe conditions

i inlet pipe conditions

r residual gas

o reference orifice in the flow test

v inlet valve in the flow-test equations

## REFERENCES

1. Livengood, James C., and Stanitz, John D.: The Effect of Inlet-Valve Design, Size, and Lift on the Air Capacity and Output of a Four-Stroke Engine. NACA TN No. 915, 1943.

2. Anon: Fluid Meters - Their Theory and Application. Pt. 1. A.S.M.E., 4th ed., 1937.

3. Taylor, C. Fayette and Taylor, Edward S.: The Internal Combustion Engine. International Textbook Co. (Scranton), 1938.

4. Nutting, E. M., and Lewis, G. W.: Air Flow through Poppet Valves. NACA Rep. No. 24, 1918.

5. Tanaka, Keikiti: Air Flow through Suction Valve of Conical Seat. Rep. No. 50 (vol. IV, no. 9), Aero. Res. Inst., Tokyo Imperial Univ., Oct. 1929.

6. Waldron, C. D.: Intermittent-Flow Coefficients of a Poppet Valve. NACA TN No. 701, 1939.

7. Wood, G. B., Jr., Hunter, D. U., Taylor, E. S., and Taylor, C. F.: Air Flow through Intake Valves. SAE Jour., vol. 50, no. 6, June 1942, pp. 212-220, 252.

TABLE I.- RESULTS OF TESTS FOR CAMSHAFT 1

[Inlet-valve diameter, 0.830 in.; inlet-valve lift, 0.208 in.; $C_{av}$, 0.445]

| Speed (rpm) | Air flow (lb/sec) | Vol. eff., e | bhp | ihp | $\phi$ |
|---|---|---|---|---|---|
| $p_i$ = 30 in. Hg; $p_e$ = 30 in. Hg | | | | | |
| 500 | 0.00581 | 0.939 | 2.37 | 2.84 | 0.1825 |
| 800 | .00903 | .911 | 3.81 | | .292 |
| 1200 | .01305 | .878 | 5.62 | | .438 |
| 1600 | .0162 | .817 | 6.75 | | .584 |
| 2000 | .0183 | .738 | 7.60 | 11.09 | .730 |
| 2400 | .0196 | .659 | 7.40 | | .876 |
| 2800 | .0201 | .580 | 7.17 | | 1.021 |
| 3200 | .0203 | .512 | 6.40 | | 1.169 |
| 3600 | .0215 | .482 | 5.75 | 12.89 | 1.313 |
| $p_i$ = 40 in. Hg; $p_e$ = 20 in. Hg | | | | | |
| 500 | 0.00895 | 1.082 | 3.99 | 4.33 | 0.1825 |
| 800 | .0135 | 1.020 | 6.50 | | .292 |
| 1200 | .01945 | .981 | 9.55 | | .438 |
| 1600 | .0245 | .926 | 12.00 | | .584 |
| 2000 | .0283 | .856 | 13.32 | 16.46 | .730 |
| 2400 | .0298 | .751 | 13.55 | | .876 |
| 2800 | .0305 | .659 | 13.10 | | 1.021 |
| 3200 | .0312 | .590 | 12.30 | | 1.169 |
| 3600 | .0328 | .551 | 11.68 | 19.65 | 1.313 |
| $p_i$ = 40 in. Hg; $p_e$ = 10 in. Hg | | | | | |
| 500 | 0.00925 | 1.120 | 4.17 | 4.40 | 0.1825 |
| 800 | .0143 | 1.081 | 6.82 | | .292 |
| 1200 | .0200 | 1.010 | 9.90 | | .438 |
| 1600 | .0252 | .953 | 12.50 | | .584 |
| 2000 | .0289 | .875 | 13.72 | 16.80 | .730 |
| 2400 | .0301 | .759 | 13.80 | | .876 |
| 2800 | .0305 | .659 | 13.32 | | 1.021 |
| 3200 | .0312 | .590 | 12.30 | | 1.169 |
| 3600 | .0335 | .563 | 12.10 | 19.45 | 1.313 |

TABLE I.- Continued

[Inlet-valve diameter, 1.05 in.; inlet-valve lift, 0.208 in.; $C_{av}$, 0.365]

| Speed (rpm) | Air flow (lb/sec) | Vol. eff., e | bhp | ihp | $\phi$ |
|---|---|---|---|---|---|
| $p_i$ = 30 in. Hg; $p_e$ = 30 in. Hg | | | | | |
| 500 | 0.00586 | 0.946 | 2.38 | 2.84 | 0.1392 |
| 800 | .00893 | .901 | 3.85 | | .223 |
| 1200 | .0133 | .894 | 5.79 | | .334 |
| 1600 | .0171 | .862 | 9.42 | | .445 |
| 2000 | .0207 | .835 | 8.85 | 12.21 | .557 |
| 2400 | .0234 | .787 | 9.50 | | .669 |
| 2800 | .0246 | .709 | 9.57 | | .780 |
| 3200 | .0255 | .643 | 9.09 | | .891 |
| 3600 | .0260 | .583 | 8.28 | 16.00 | 1.002 |
| $p_i$ = 40 in. Hg; $p_e$ = 20 in. Hg | | | | | |
| 500 | 0.009 | 1.090 | 3.91 | 4.24 | 0.1392 |
| 800 | .0138 | 1.043 | 6.52 | | .223 |
| 1200 | .02005 | 1.011 | 9.87 | | .334 |
| 1600 | .0257 | .972 | 12.90 | | .445 |
| 2000 | .0308 | .932 | 14.50 | 18.20 | .557 |
| 2400 | .0343 | .865 | 15.83 | | .669 |
| 2800 | .0363 | .785 | 16.09 | | .780 |
| 3200 | .0376 | .710 | 15.61 | | .891 |
| 3600 | .0399 | .670 | 15.50 | 23.75 | 1.002 |
| $p_i$ = 40 in. Hg; $p_e$ = 10 in. Hg | | | | | |
| 500 | 0.00928 | 1.122 | 4.10 | 4.35 | 0.1392 |
| 800 | .01415 | 1.070 | 6.78 | | .223 |
| 1200 | .0205 | 1.034 | 10.26 | | .334 |
| 1600 | .0264 | .998 | 13.38 | | .445 |
| 2000 | .0317 | .959 | 15.05 | 18.90 | .557 |
| 2400 | .0351 | .885 | 16.13 | | .669 |
| 2800 | .0367 | .793 | 16.25 | | .780 |
| 3200 | .0379 | .716 | 15.75 | | .891 |
| 3600 | .0399 | .670 | 15.62 | 24.20 | 1.002 |

TABLE I.- Concluded

[Inlet-valve diameter, 1.05 in.; inlet-valve lift, 0.262 in.; $C_{av}$, 0.445]

| Speed (rpm) | Air flow (lb/sec) | Vol. eff., e | bhp | ihp | $\phi$ |
|---|---|---|---|---|---|
| $p_i$ = 30 in. Hg; $p_e$ = 30 in. Hg | | | | | |
| 500 | 0.00586 | 0.946 | 2.37 | 2.84 | 0.1142 |
| 800 | .00885 | .893 | 3.64 | | .1828 |
| 1200 | .01295 | .871 | 5.38 | | .274 |
| 1600 | .0172 | .868 | 7.20 | | .366 |
| 2000 | .0215 | .867 | 9.09 | 12.60 | .457 |
| 2400 | .0248 | .834 | 10.22 | | .548 |
| 2800 | .0270 | .778 | 10.78 | | .640 |
| 3200 | .0288 | .726 | 10.70 | | .731 |
| 3600 | .0300 | .673 | 9.94 | 18.25 | .822 |
| $p_i$ = 40 in. Hg; $p_e$ = 20 in. Hg | | | | | |
| 500 | 0.00899 | 1.088 | 3.85 | 4.25 | 0.1142 |
| 800 | .01405 | 1.062 | 6.40 | | .1828 |
| 1200 | .0204 | 1.029 | 9.88 | | .274 |
| 1600 | .0265 | 1.002 | 12.80 | | .366 |
| 2000 | .0330 | .999 | 15.80 | 19.70 | .457 |
| 2400 | .0382 | .963 | 17.95 | | .548 |
| 2800 | .0418 | .903 | 19.02 | | .640 |
| 3200 | .0445 | .842 | 19.48 | | .731 |
| 3600 | .0462 | .777 | 18.80 | 28.00 | .822 |
| $p_i$ = 40 in. Hg; $p_e$ = 10 in. Hg | | | | | |
| 500 | 0.0093 | 1.128 | 4.04 | 4.28 | 0.1142 |
| 800 | .0142 | 1.073 | 6.66 | | .1828 |
| 1200 | .0207 | 1.043 | 10.25 | | .274 |
| 1600 | .0271 | 1.025 | 13.38 | | .366 |
| 2000 | .0337 | 1.020 | 16.50 | 19.70 | .457 |
| 2400 | .0389 | .980 | 18.48 | | .548 |
| 2800 | .0425 | .918 | 19.50 | | .640 |
| 3200 | .0450 | .851 | 19.60 | | .731 |
| 3600 | .0467 | .785 | 19.10 | 28.60 | .822 |

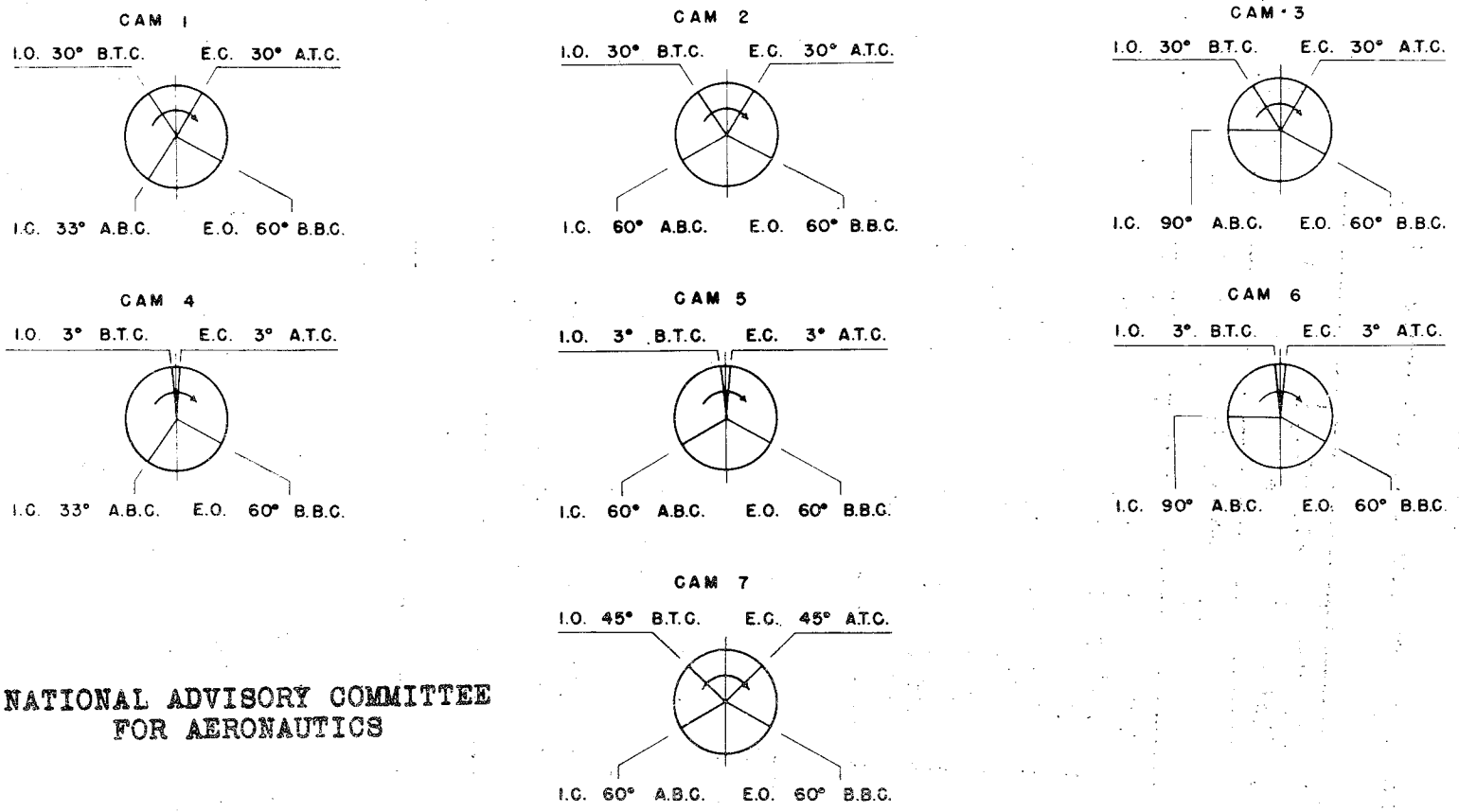


NATIONAL ADVISORY COMMITTEE
FOR AERONAUTICS

Figure 1.- Timing diagrams for the camshafts used in the tests.

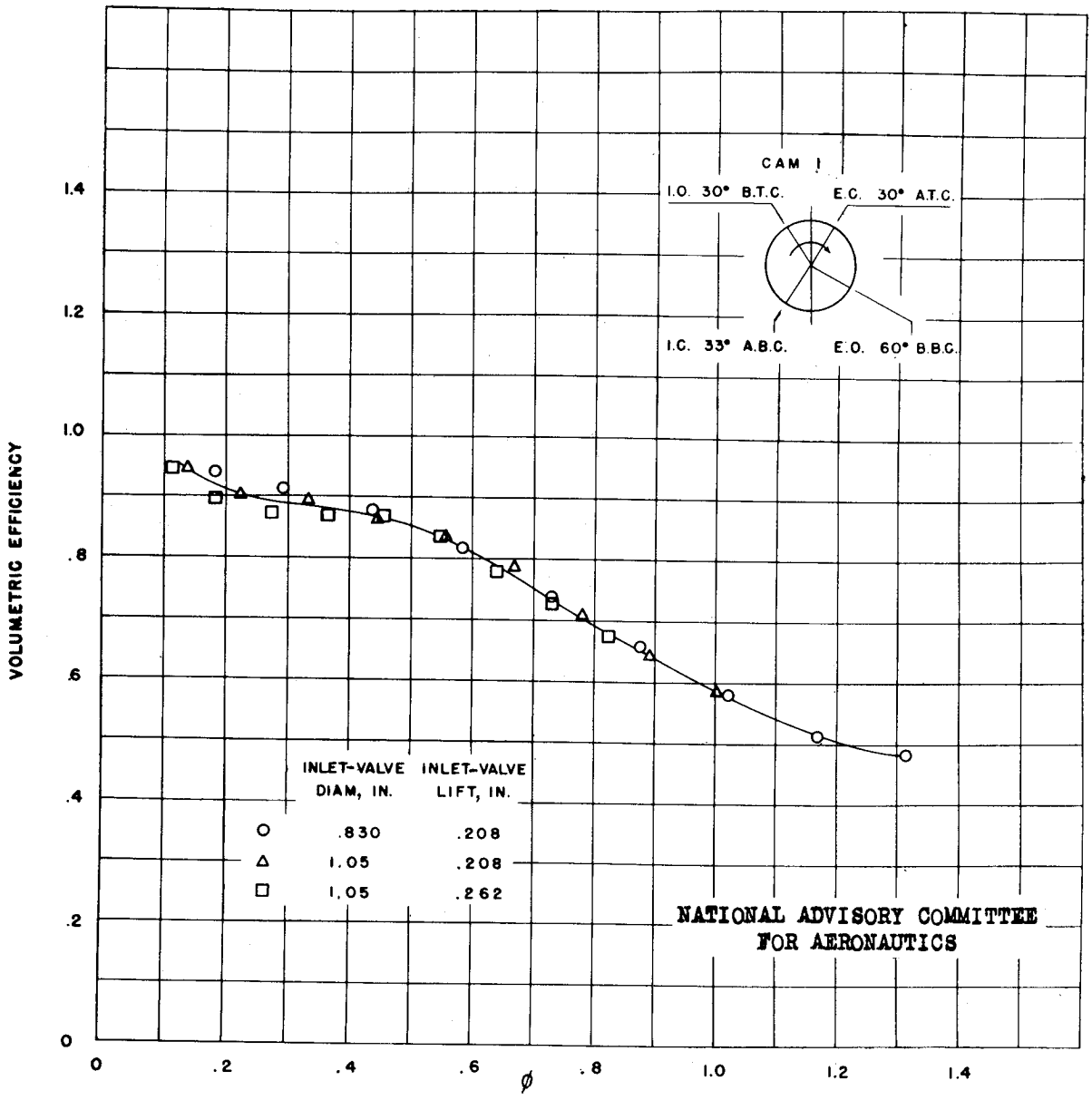


Figure 2.- Volumetric efficiency against ø. Camshaft 1; $p_i$ = 30, $p_e$ = 30 inches of mercury.

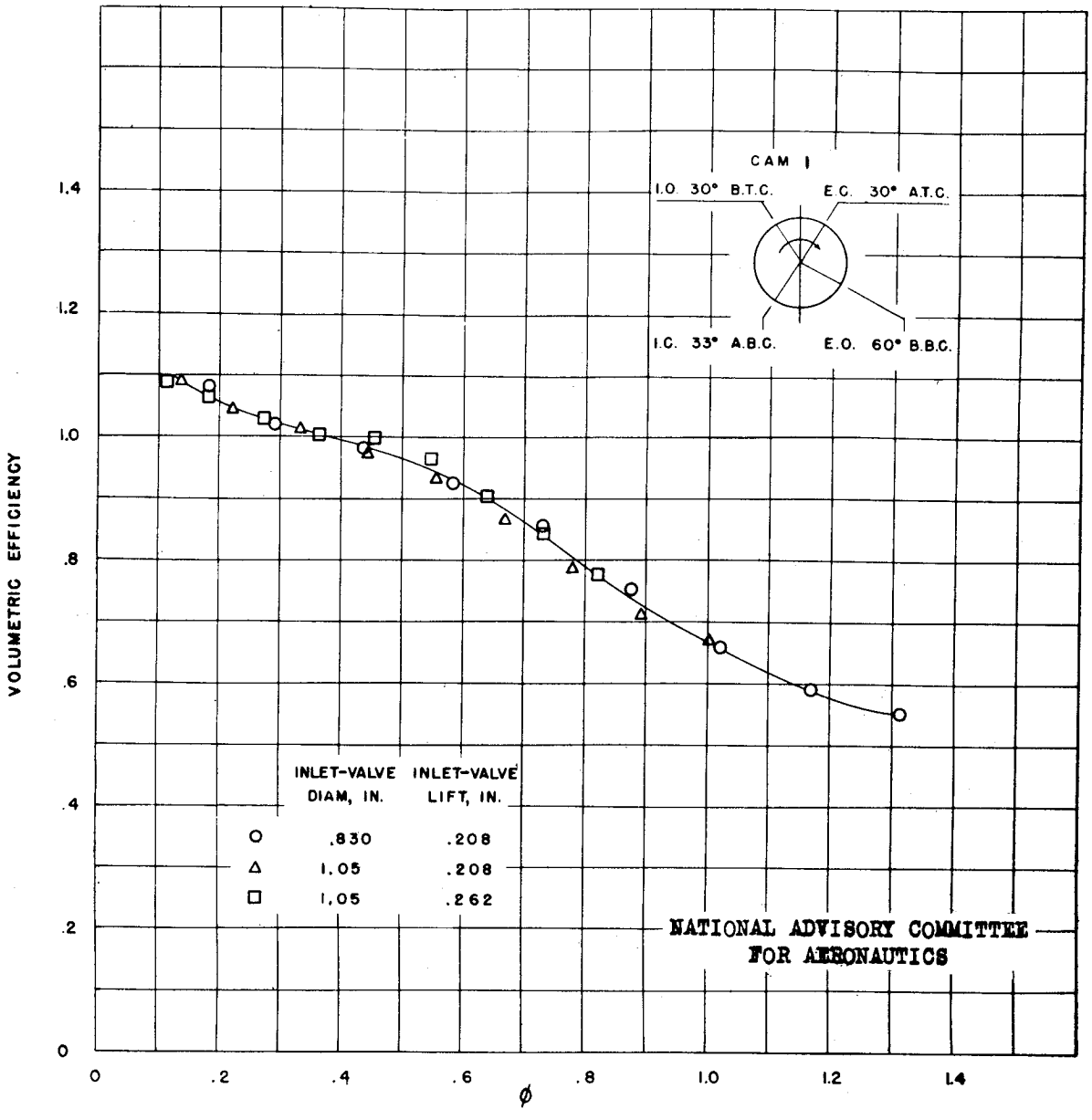


Figure 3.- Volumetric efficiency against ϕ. Camshaft 1; $p_i$ = 40, $p_e$ = 20 inches of mercury.

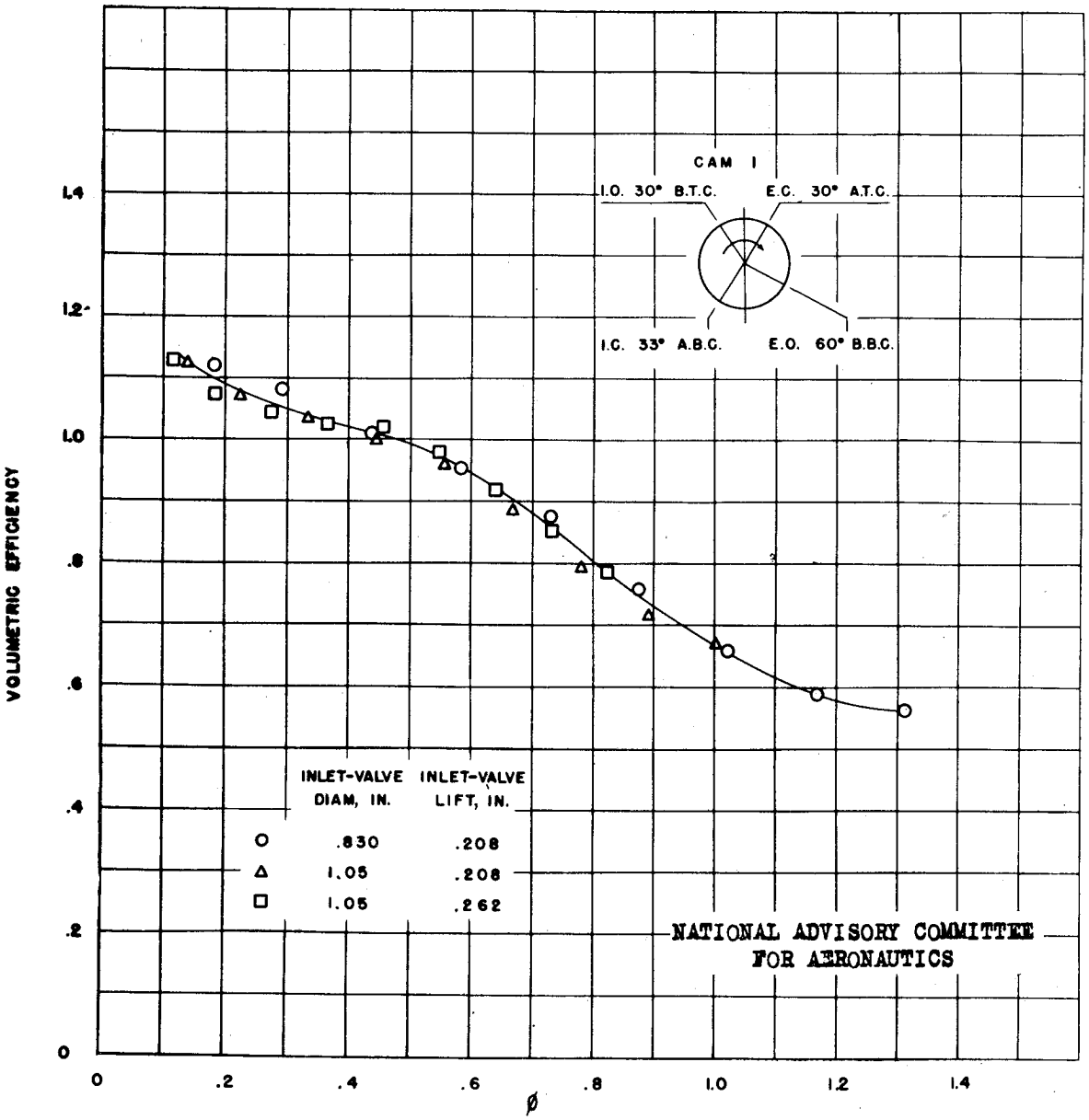


Figure 4.- Volumetric efficiency against ø. Camshaft 1; $p_i$ = 40, $p_e$ = 10 inches of mercury.

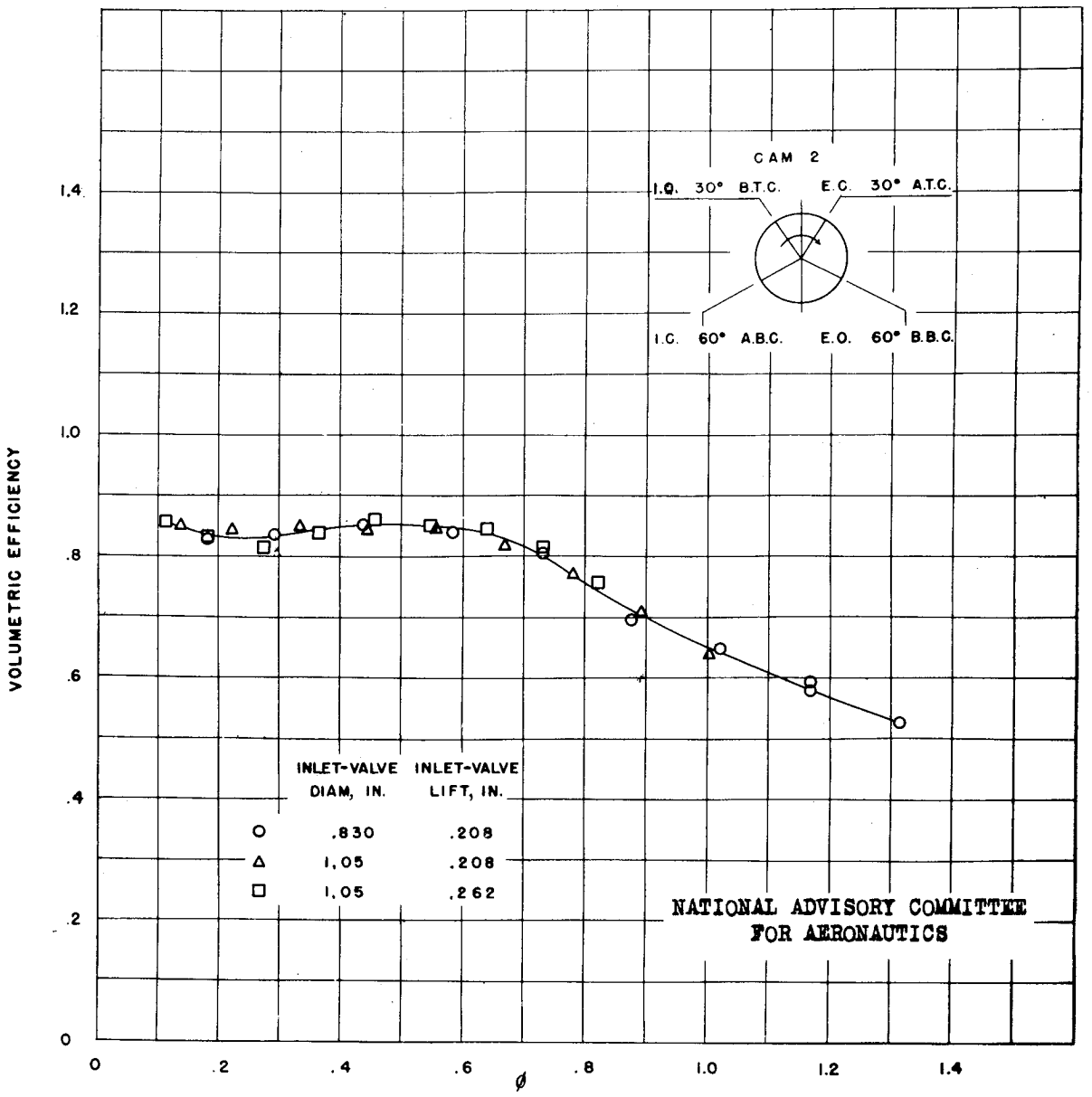


Figure 5.- Volumetric efficiency against ø. Camshaft 2; $p_i$ = 30, $p_e$ = 30 inches of mercury.

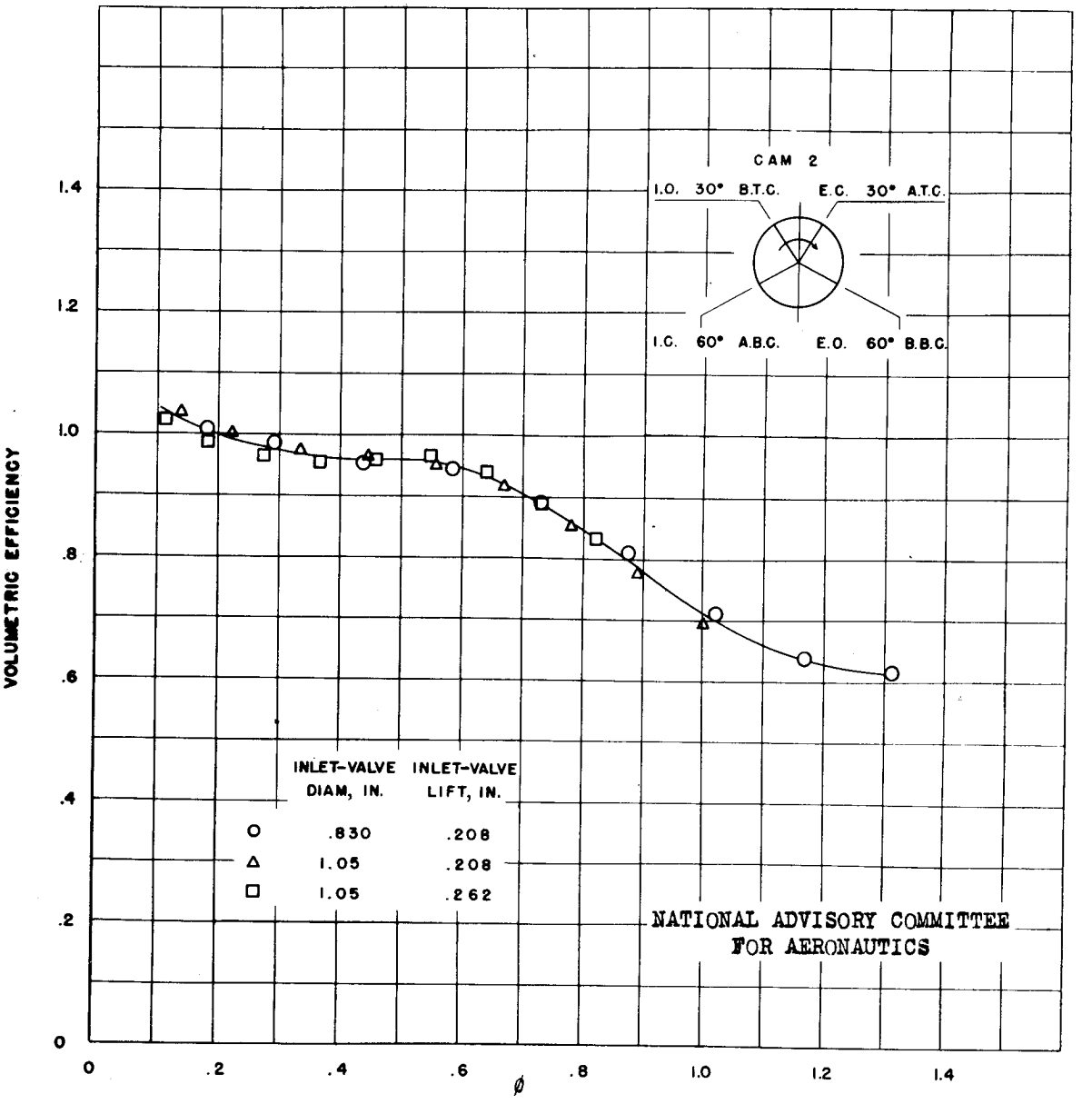


Figure 6.- Volumetric efficiency against ø. Camshaft 2; $p_i$ = 40, $p_e$ = 20 inches of mercury.

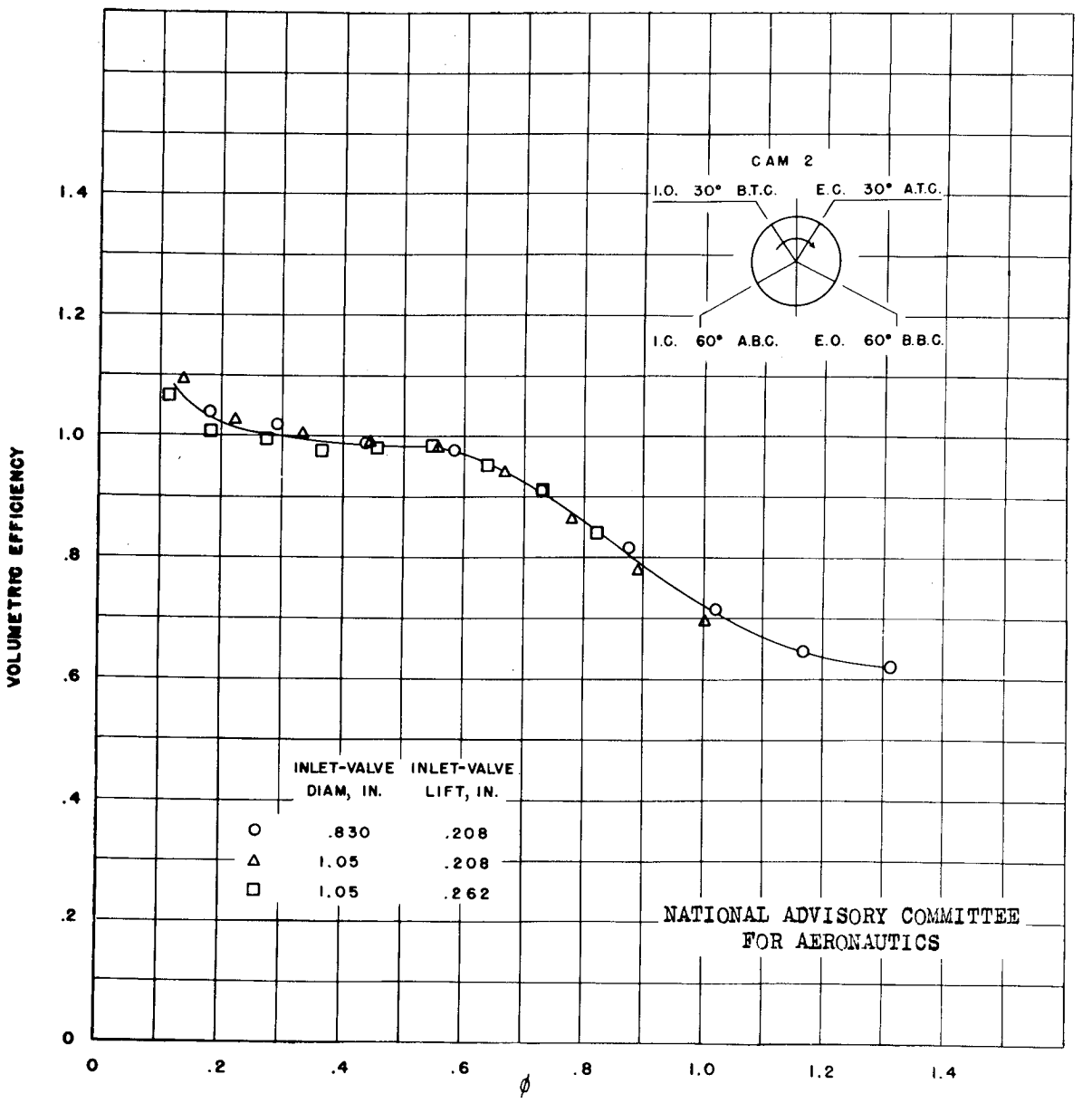


Figure 7.- Volumetric efficiency against ϕ. Camshaft 2; $p_i$ = 40, $p_e$ = 10 inches of mercury.

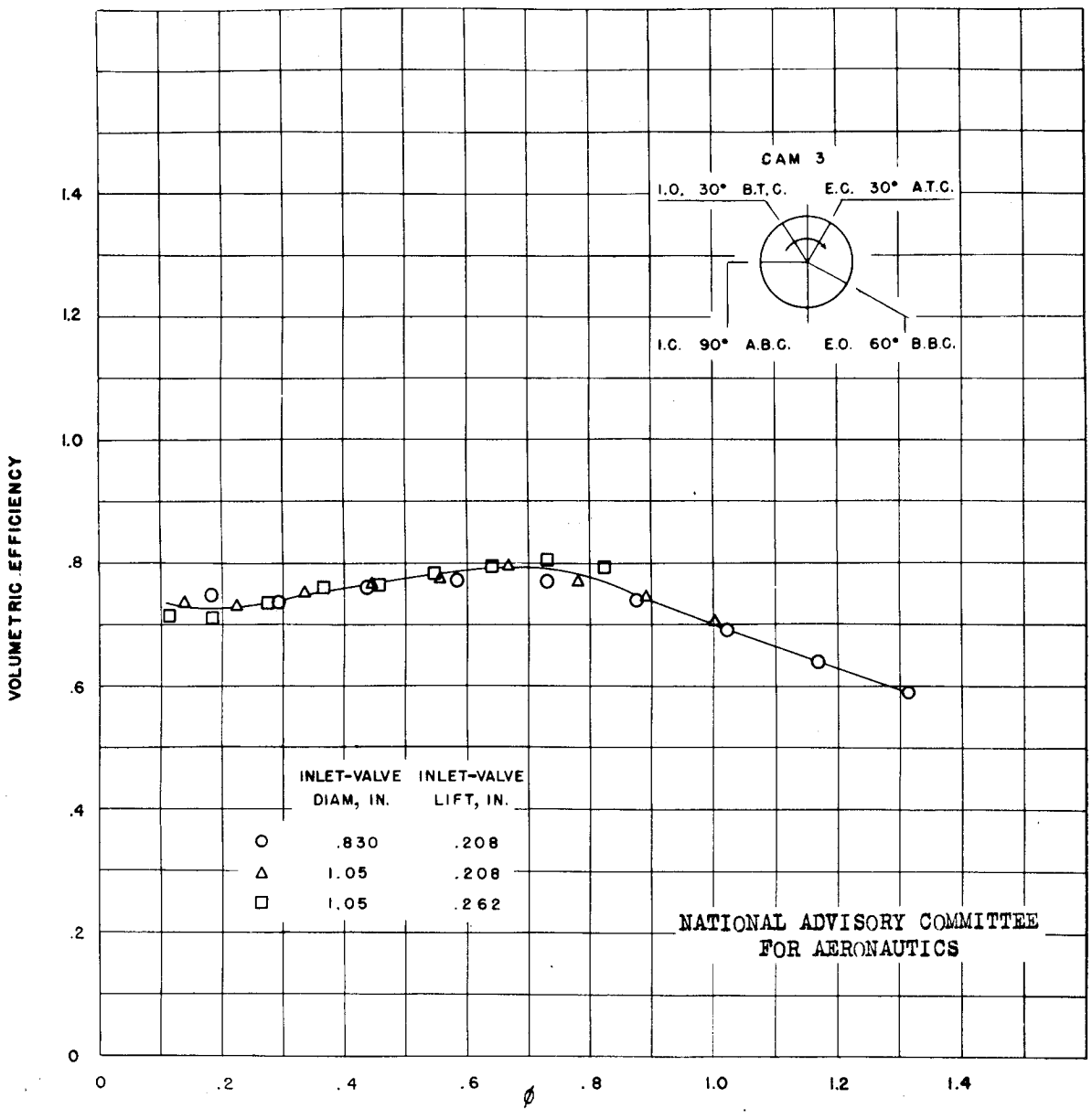


Figure 8.- Volumetric efficiency against ϕ. Camshaft 3; $p_i$ = 30, $p_e$ = 30 inches of mercury.

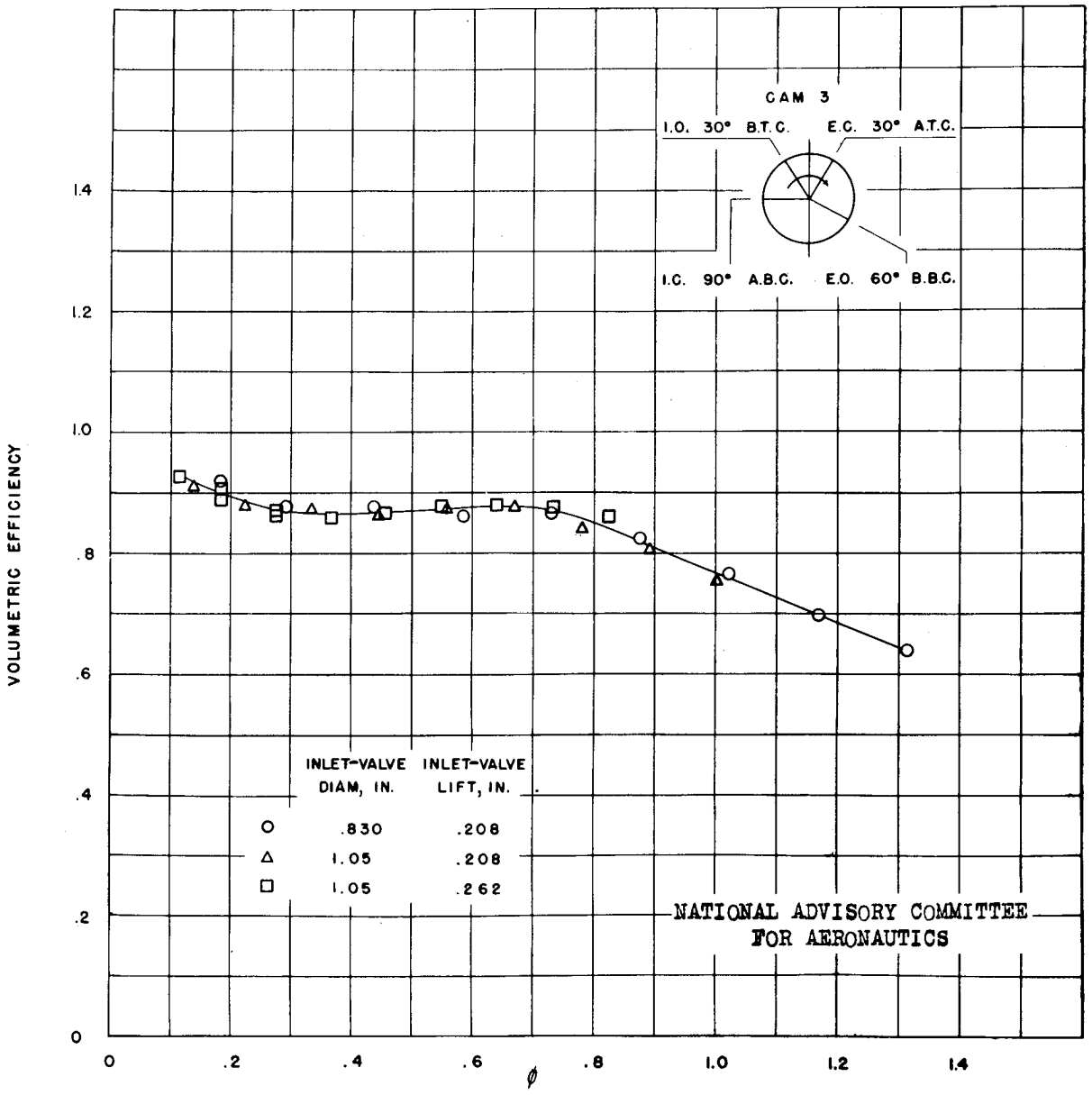


Figure 9.- Volumetric efficiency against ϕ. Camshaft 3; $p_i$ = 40, $p_e$ = 20 inches of mercury.

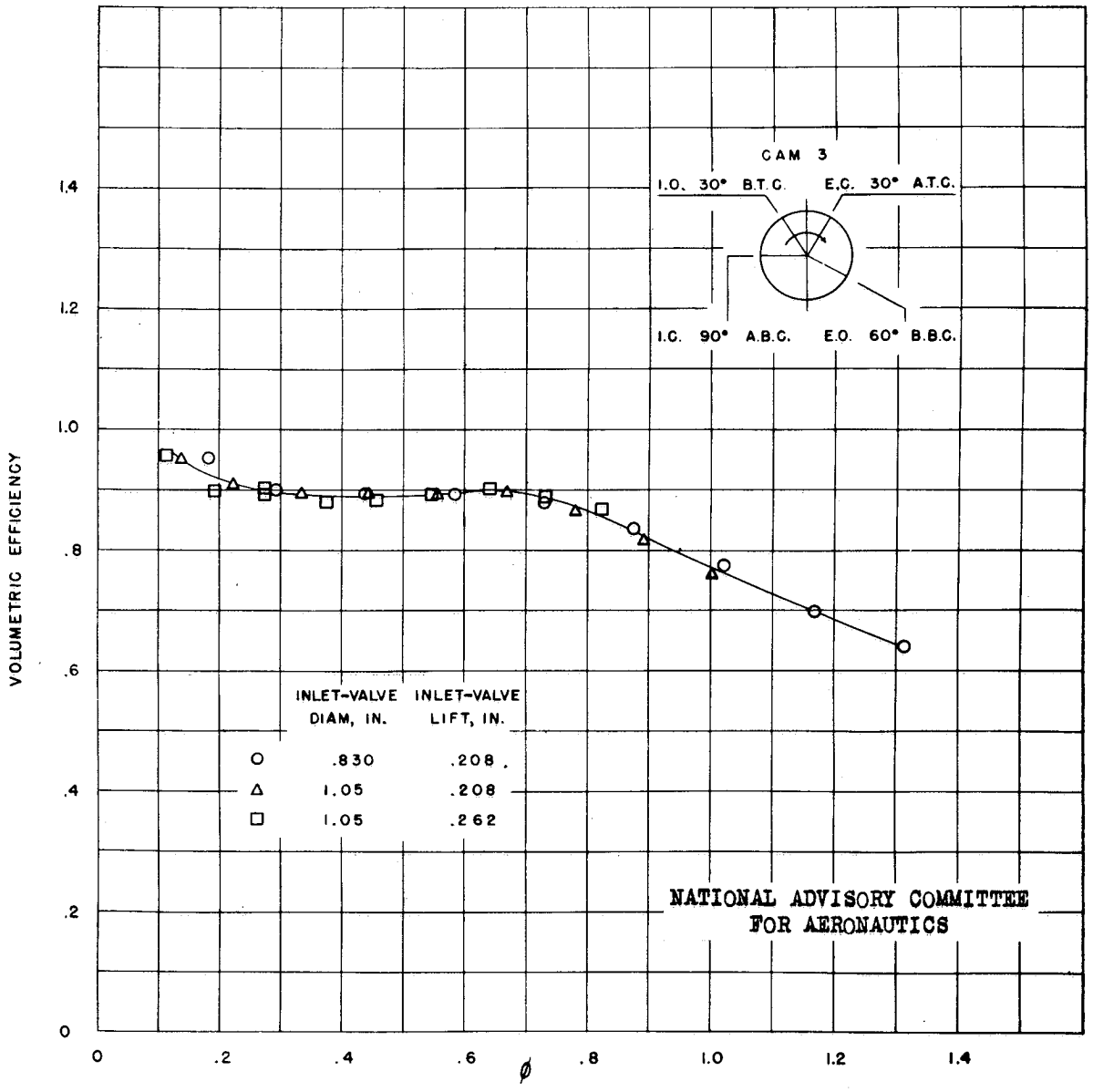


Figure 10.- Volumetric efficiency against ϕ. Camshaft 3; $p_i$ = 40, $p_e$ = 10 inches of mercury.

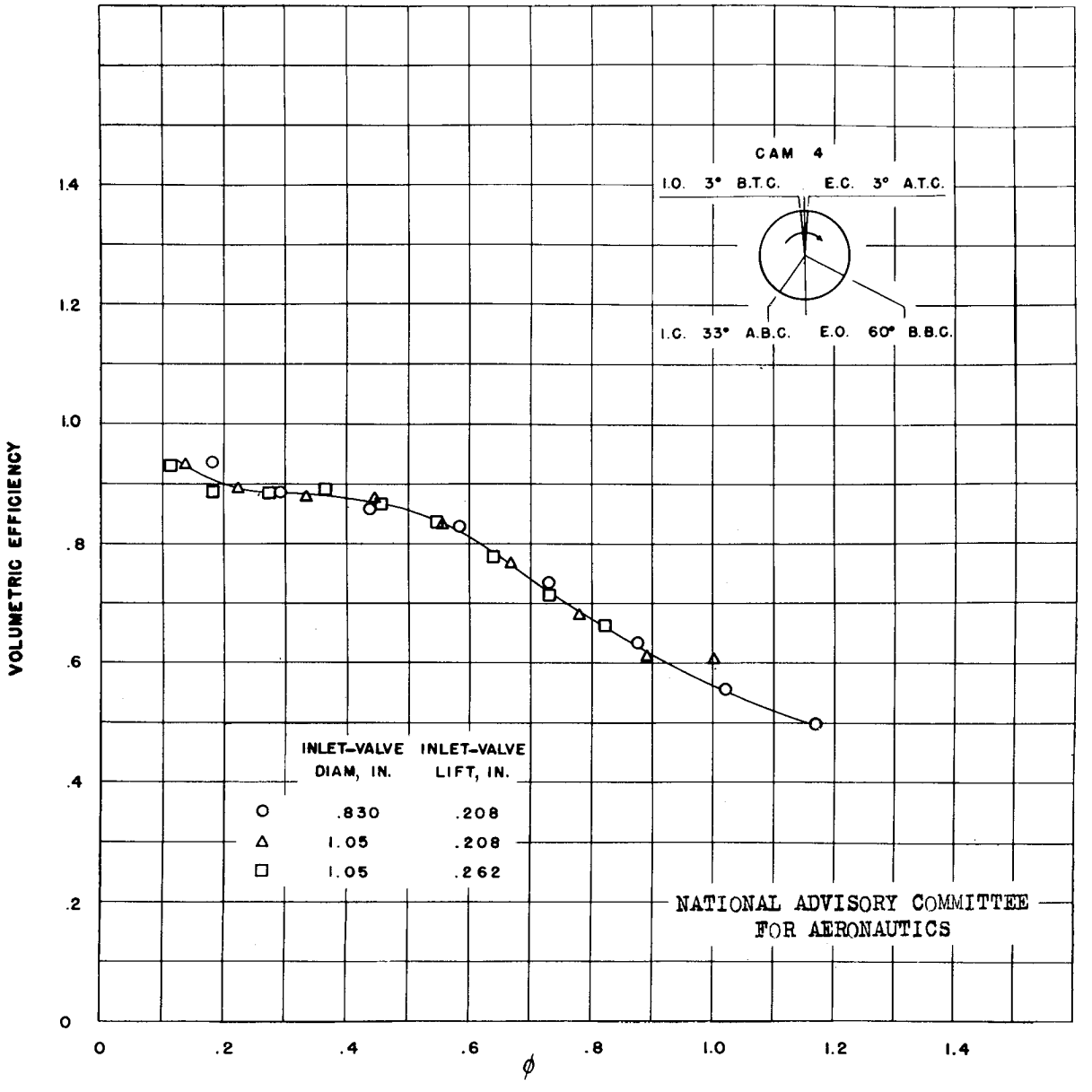


Figure 11.- Volumetric efficiency against ϕ. Camshaft 4; $p_i$ = 30, $p_e$ = 30 inches of mercury.

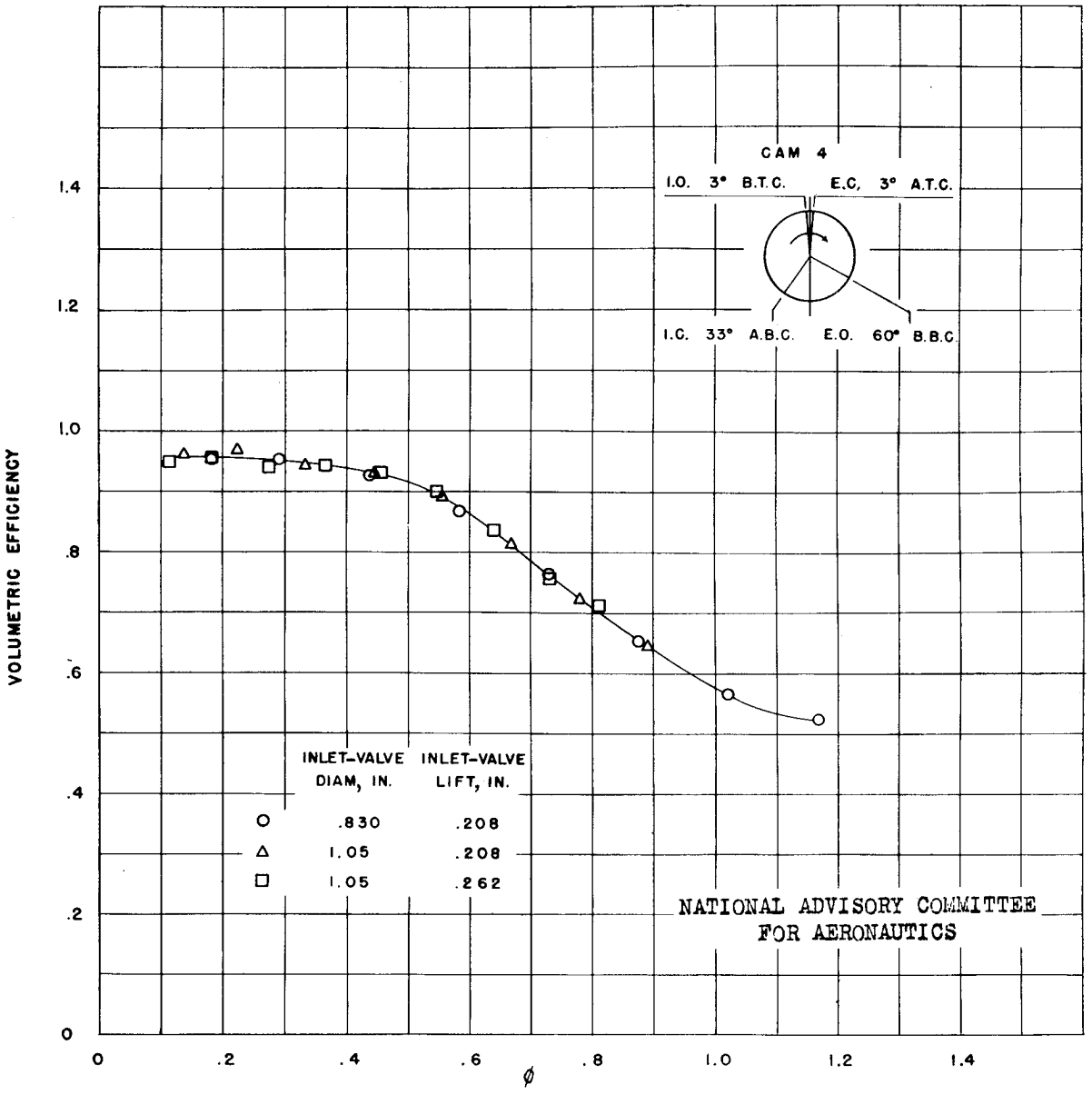


Figure 12.- Volumetric efficiency against ϕ. Camshaft 4; $p_i$ = 40, $p_e$ = 20 inches of mercury.

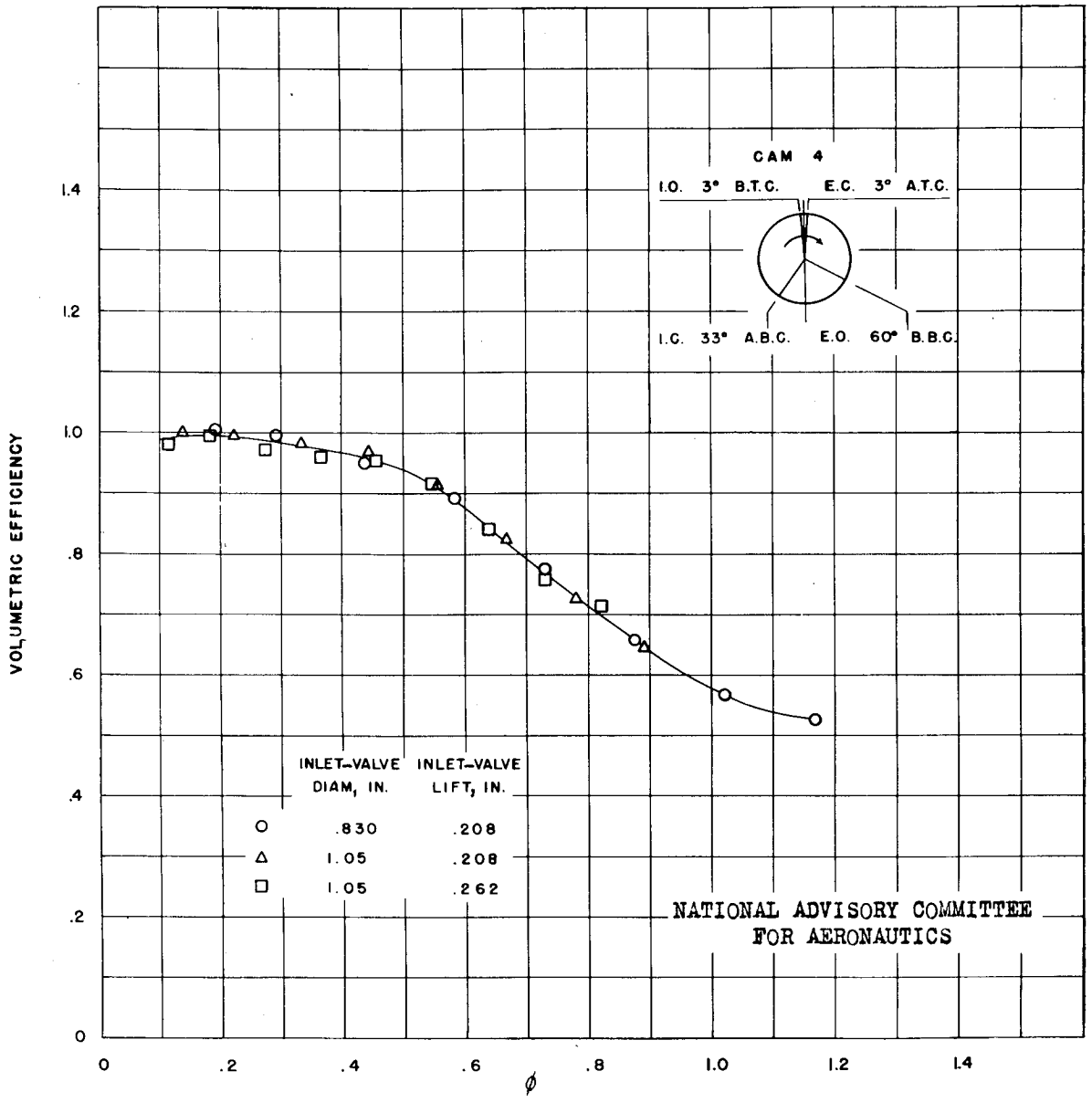


Figure 13.- Volumetric efficiency against ϕ. Camshaft 4; $p_i$ = 40, $p_e$ = 10 inches of mercury.

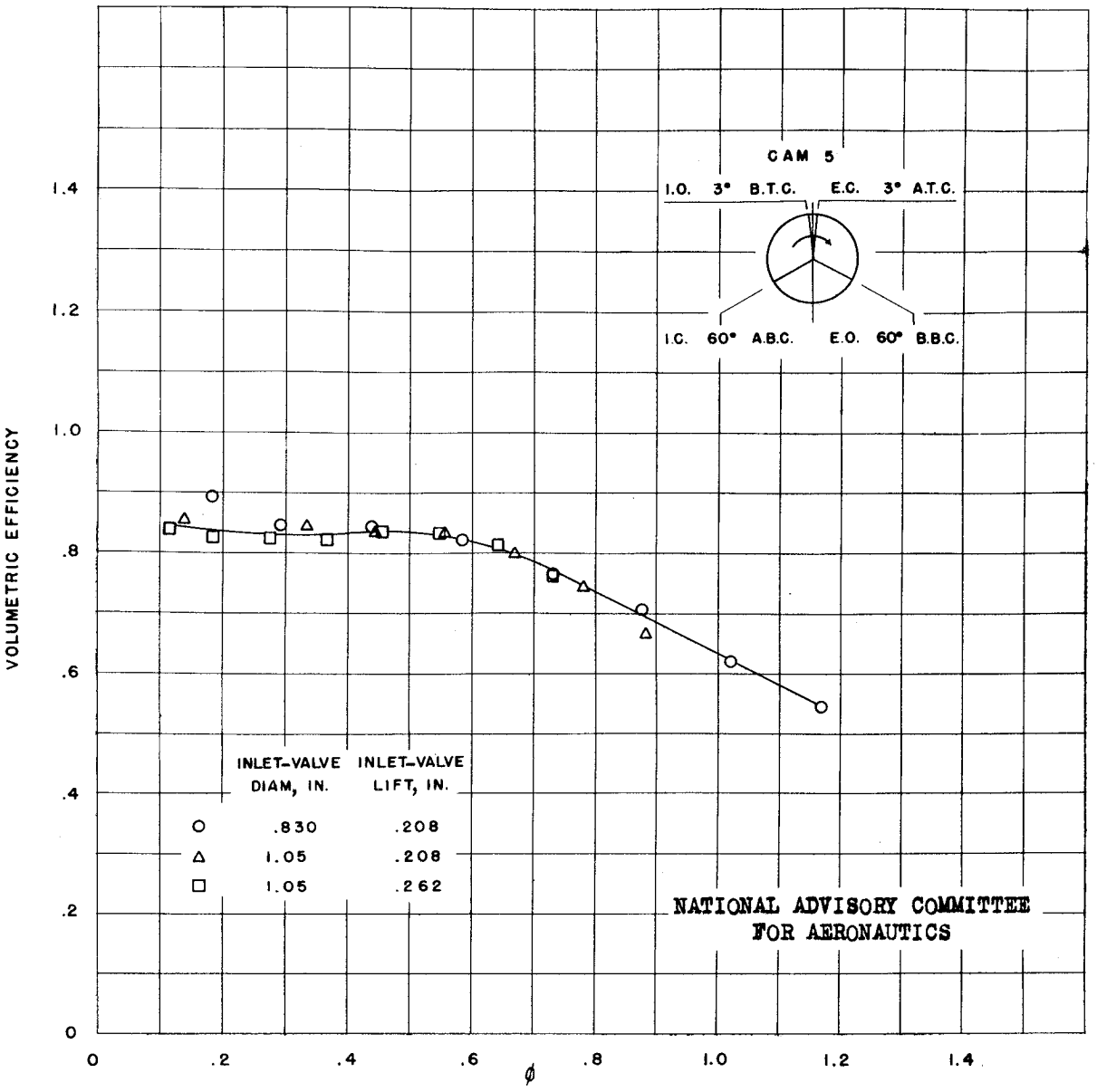


Figure 14.- Volumetric efficiency against Ø. Camshaft 5; $p_i$ = 30, $p_e$ = 30 inches of mercury.

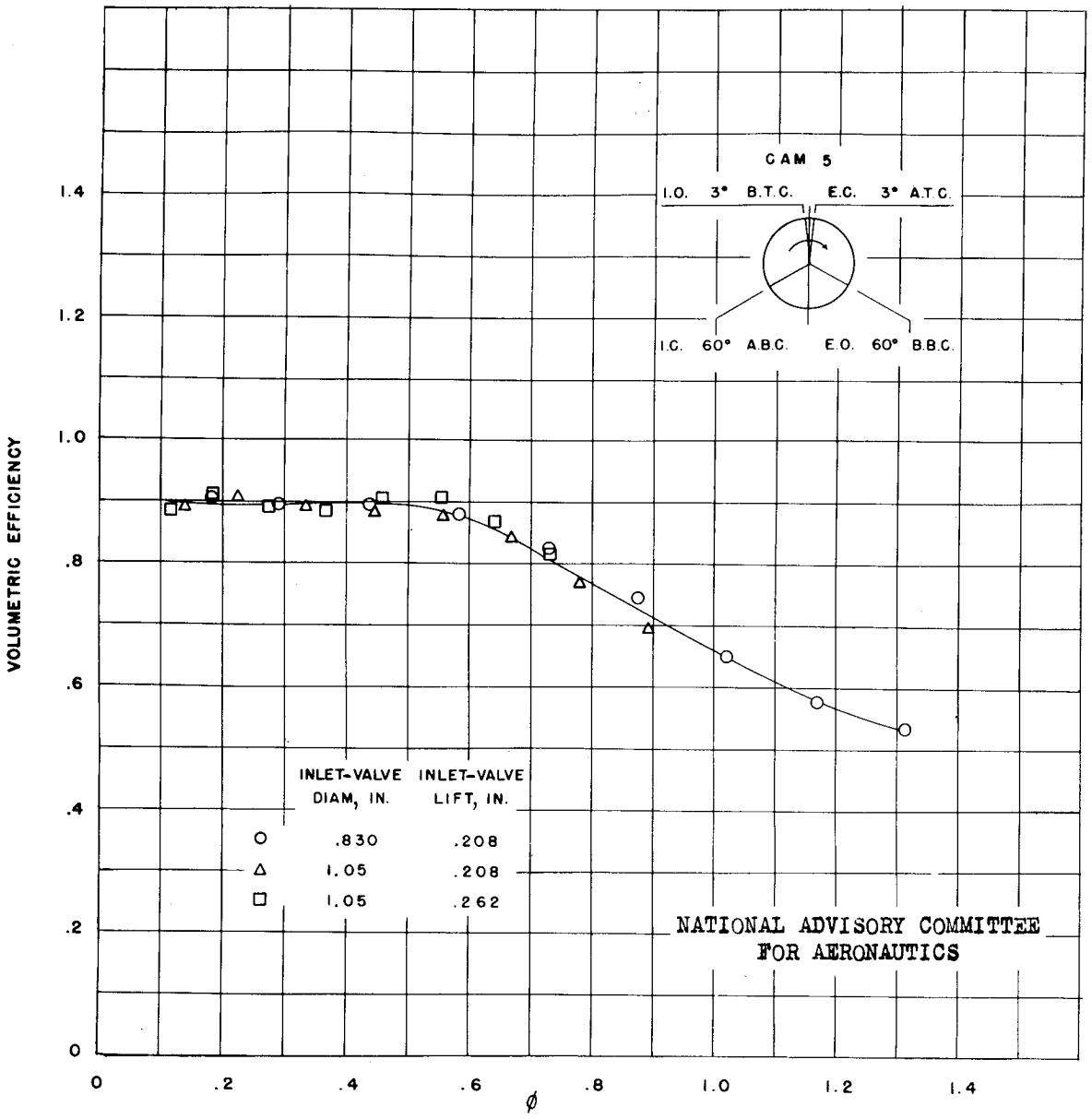


Figure 15.- Volumetric efficiency against ϕ. Camshaft 5; $p_i$ = 40, $p_e$ = 20 inches of mercury.

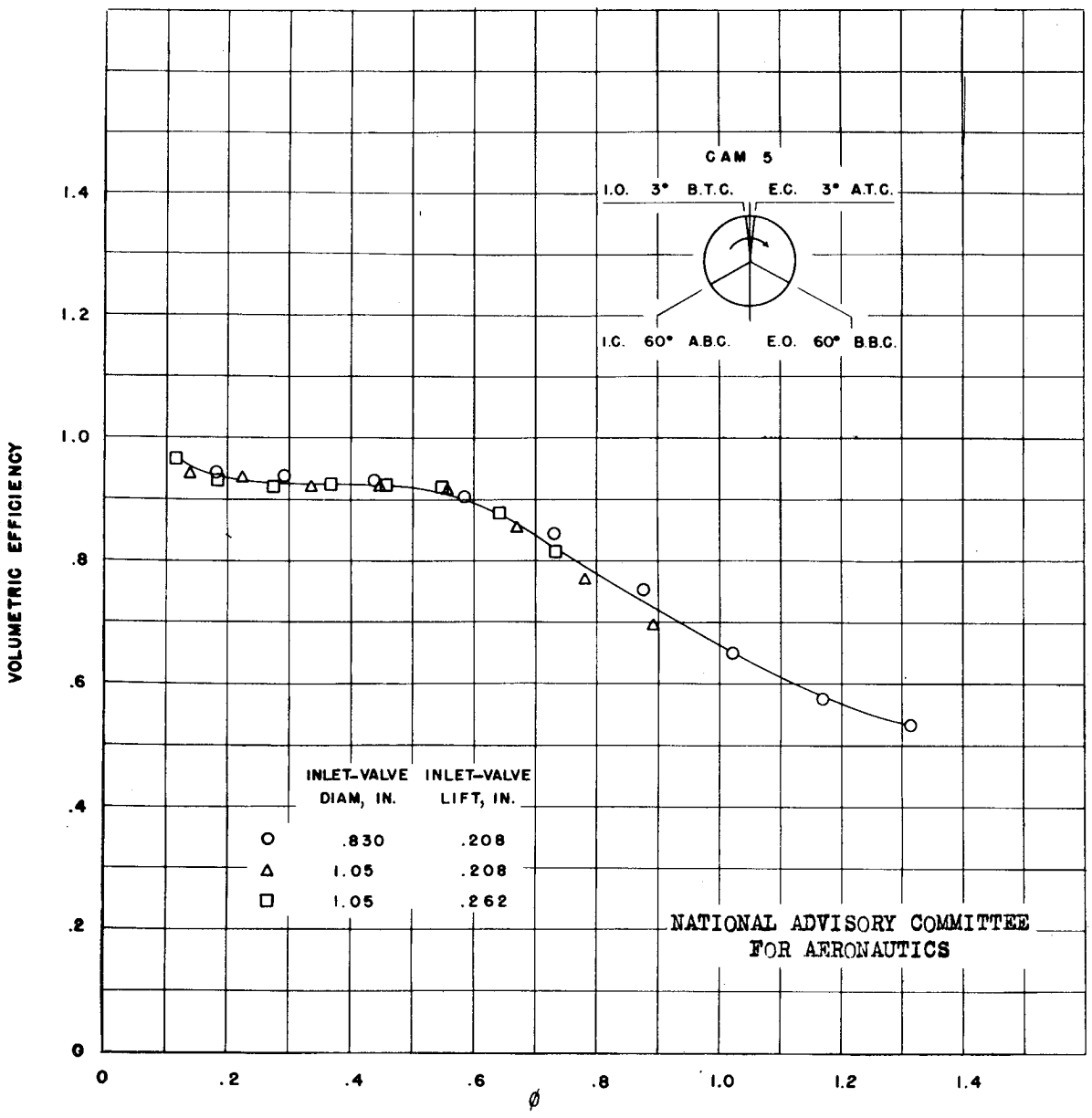


Figure 16.- Volumetric efficiency against ϕ. Camshaft 5; $p_i$ = 40, $p_e$ = 10 inches of mercury.

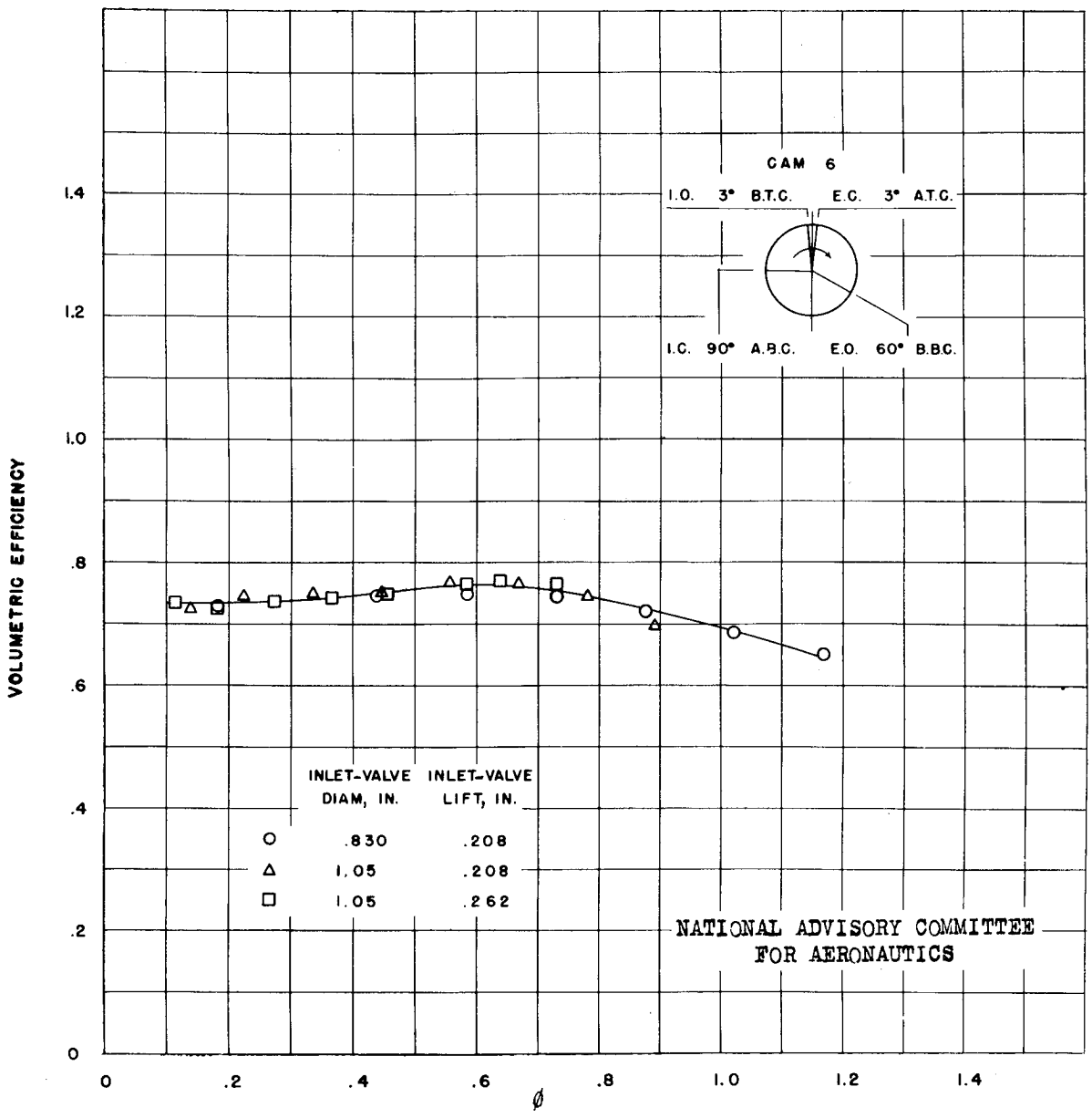


Figure 17.- Volumetric efficiency against ø. Camshaft 6; $p_i$ = 30, $p_e$ = 30 inches of mercury.

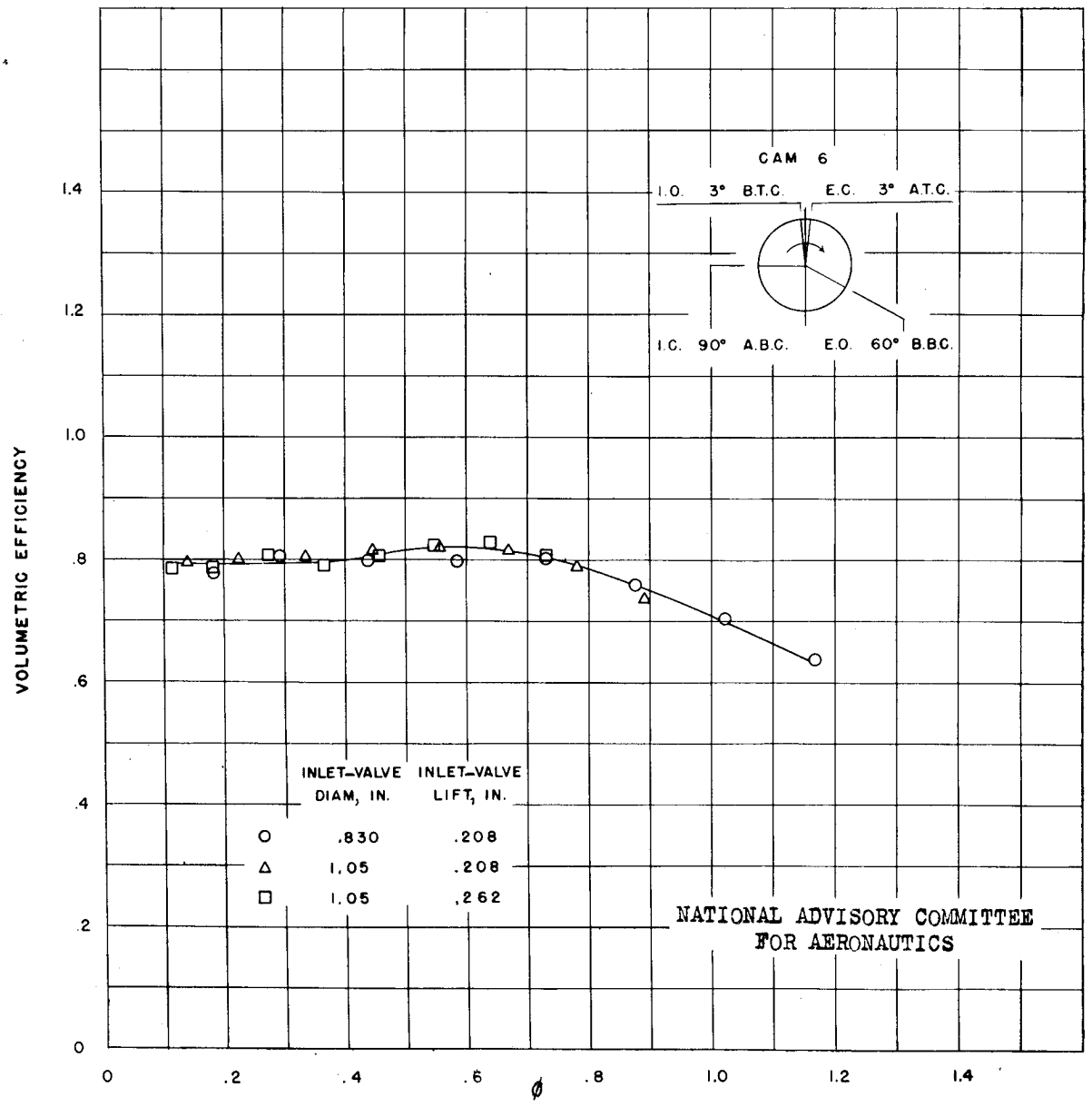


Figure 18.- Volumetric efficiency against $\phi$. Camshaft 6; $p_i$ = 40, $p_e$ = 20 inches of mercury.

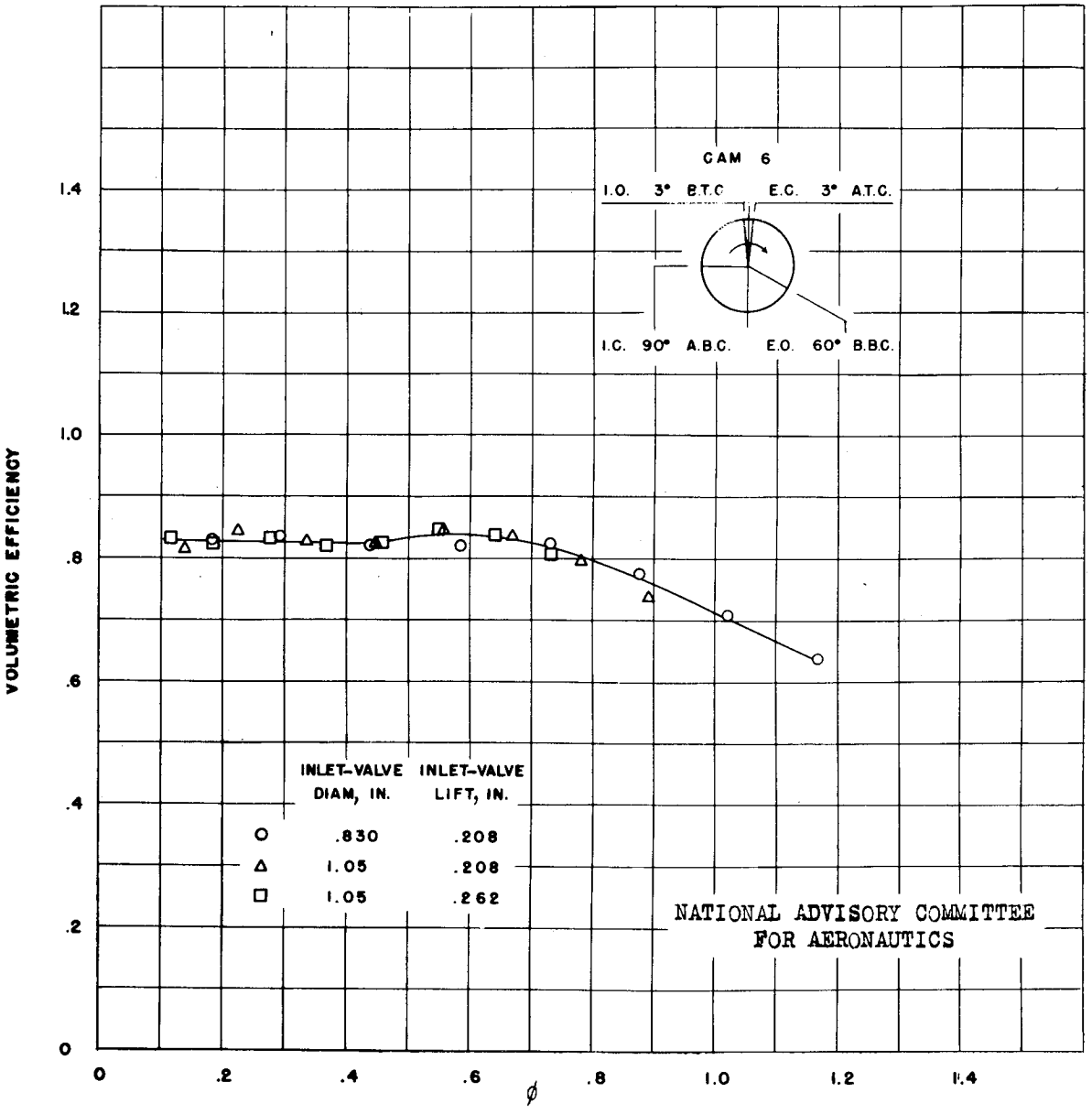


Figure 19.- Volumetric efficiency against ϕ. Camshaft 6; $p_i$ = 40, $p_e$ = 10 inches of mercury.

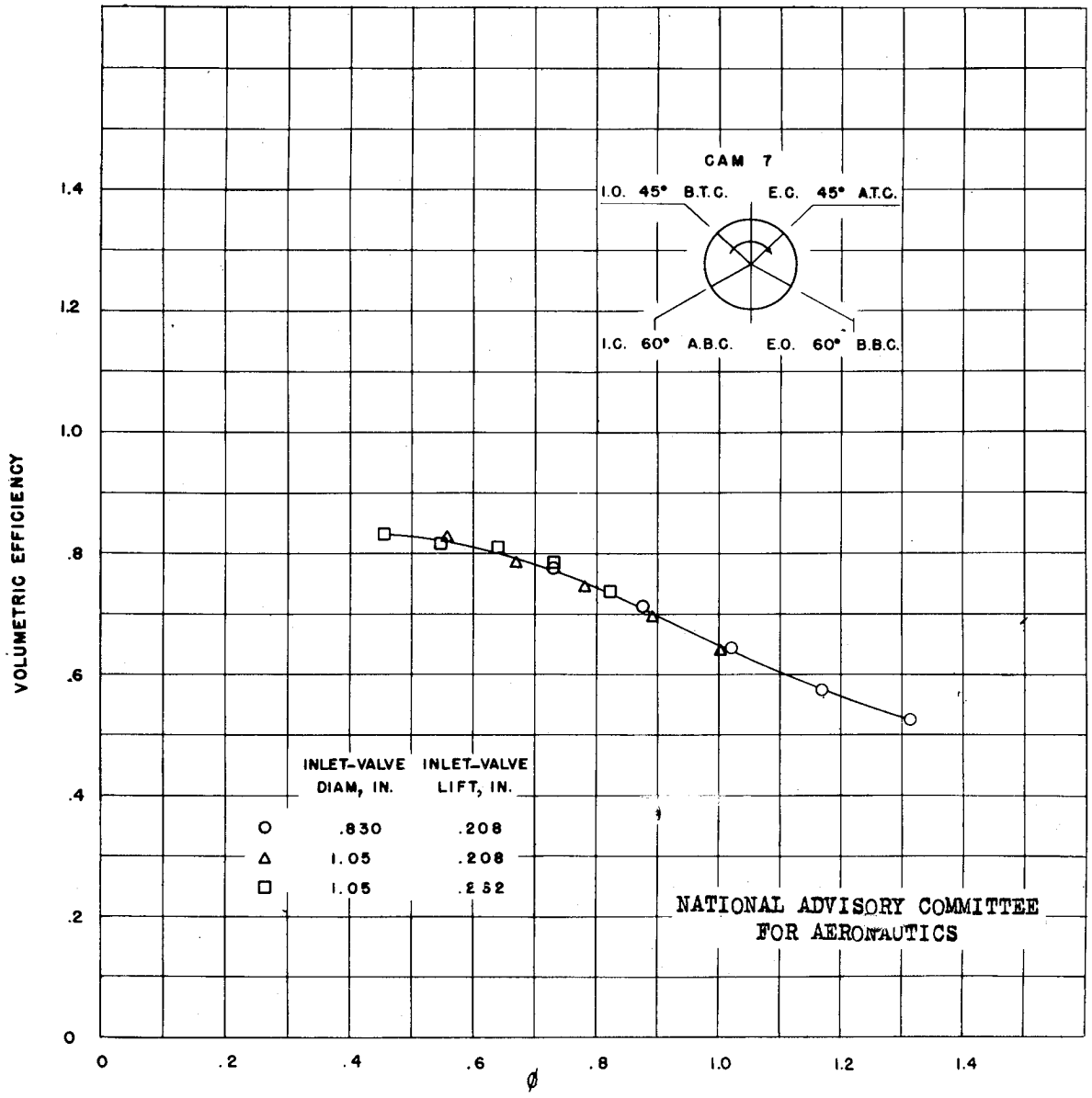


Figure 20.- Volumetric efficiency against ϕ. Camshaft 7; $p_i$ = 30, $p_e$ = 30 inches of mercury.

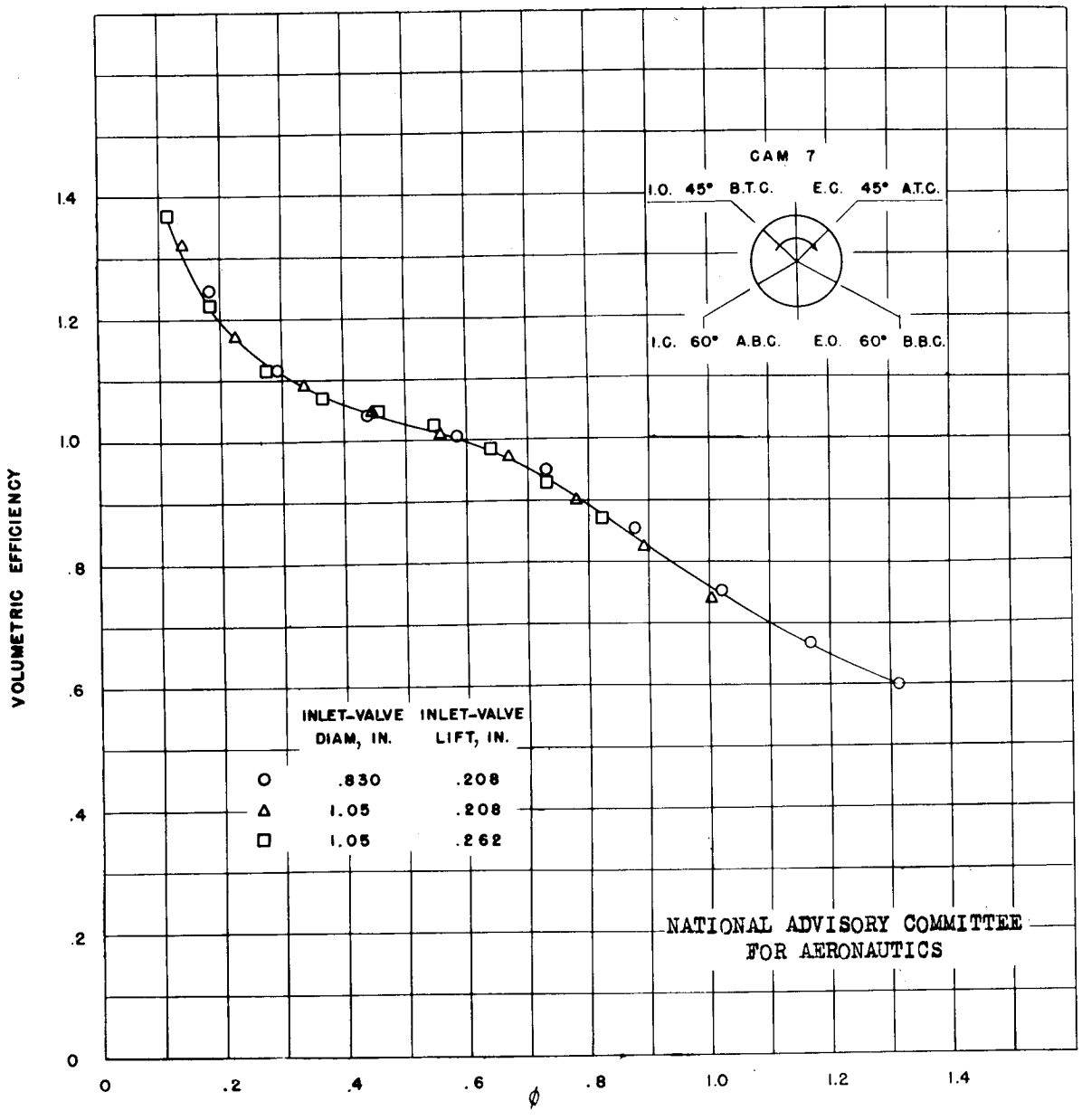


Figure 21.- Volumetric efficiency against Ø. Camshaft 7; $p_i$ = 40, $p_e$ = 20 inches of mercury.

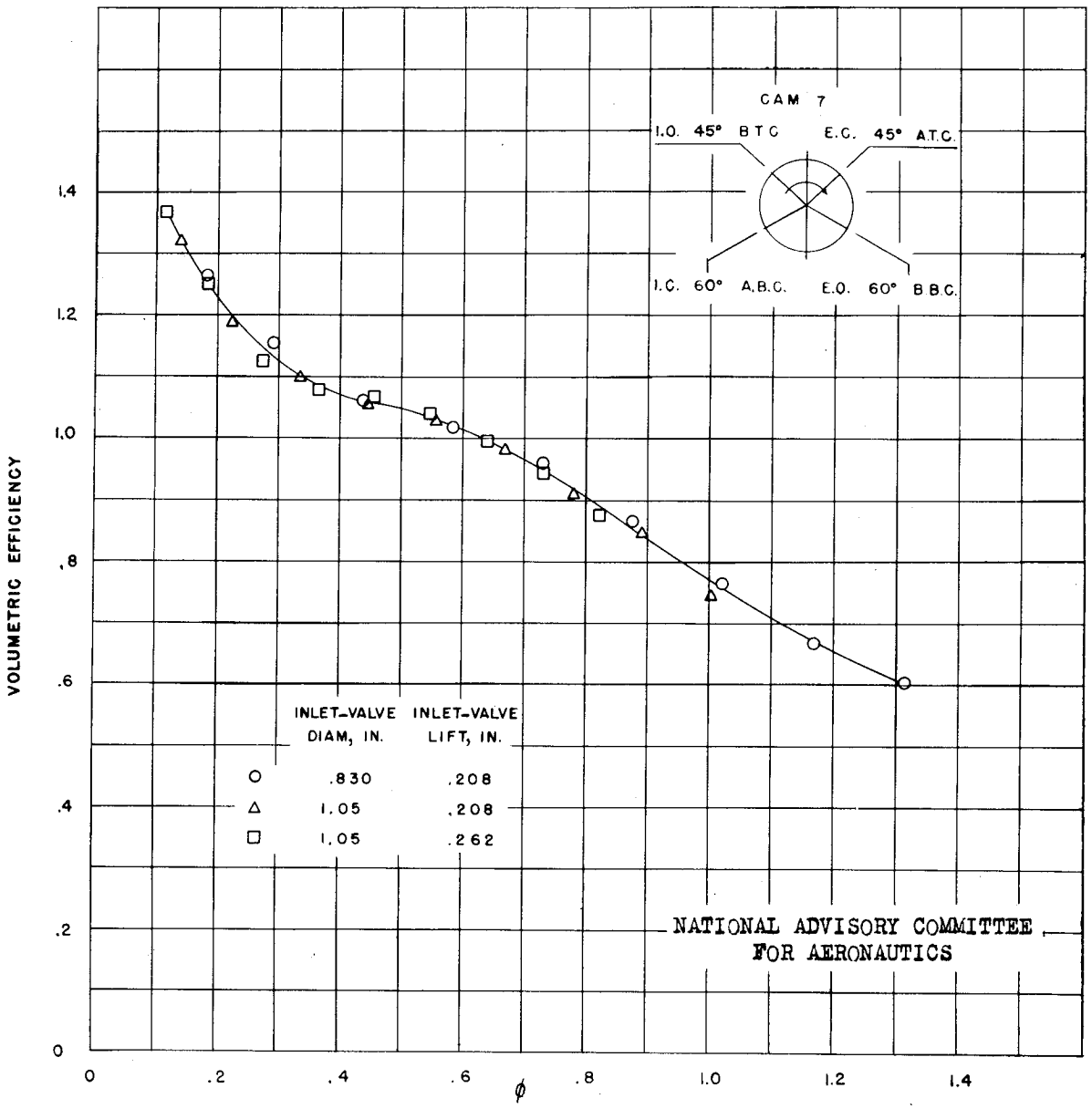


Figure 22.- Volumetric efficiency against Ø. Camshaft 7; $p_i$ = 40, $p_e$ = 10 inches of mercury.

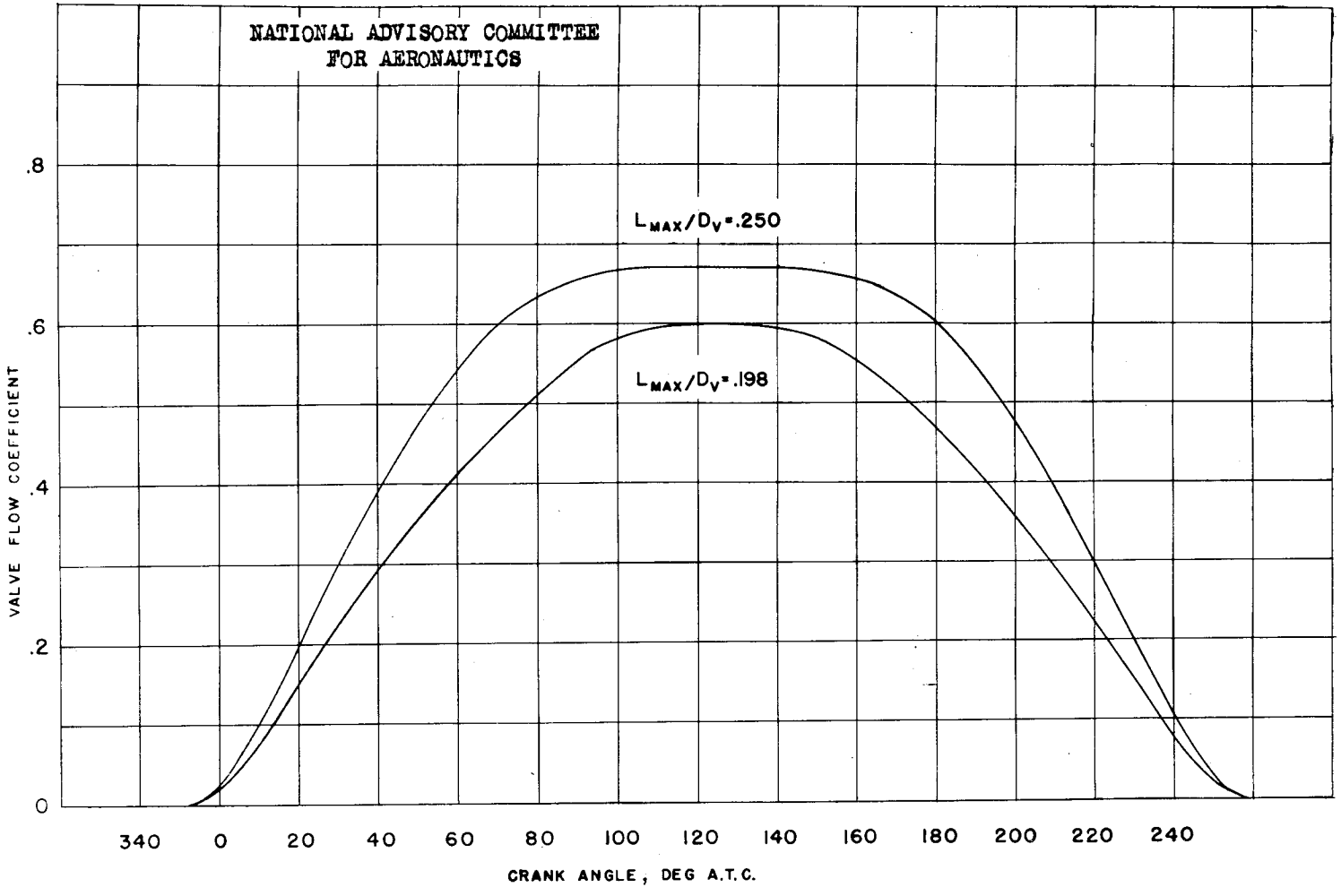


Figure 23.- Curves of flow coefficient against crank angle for the inlet-valve diameters and lifts which were used.

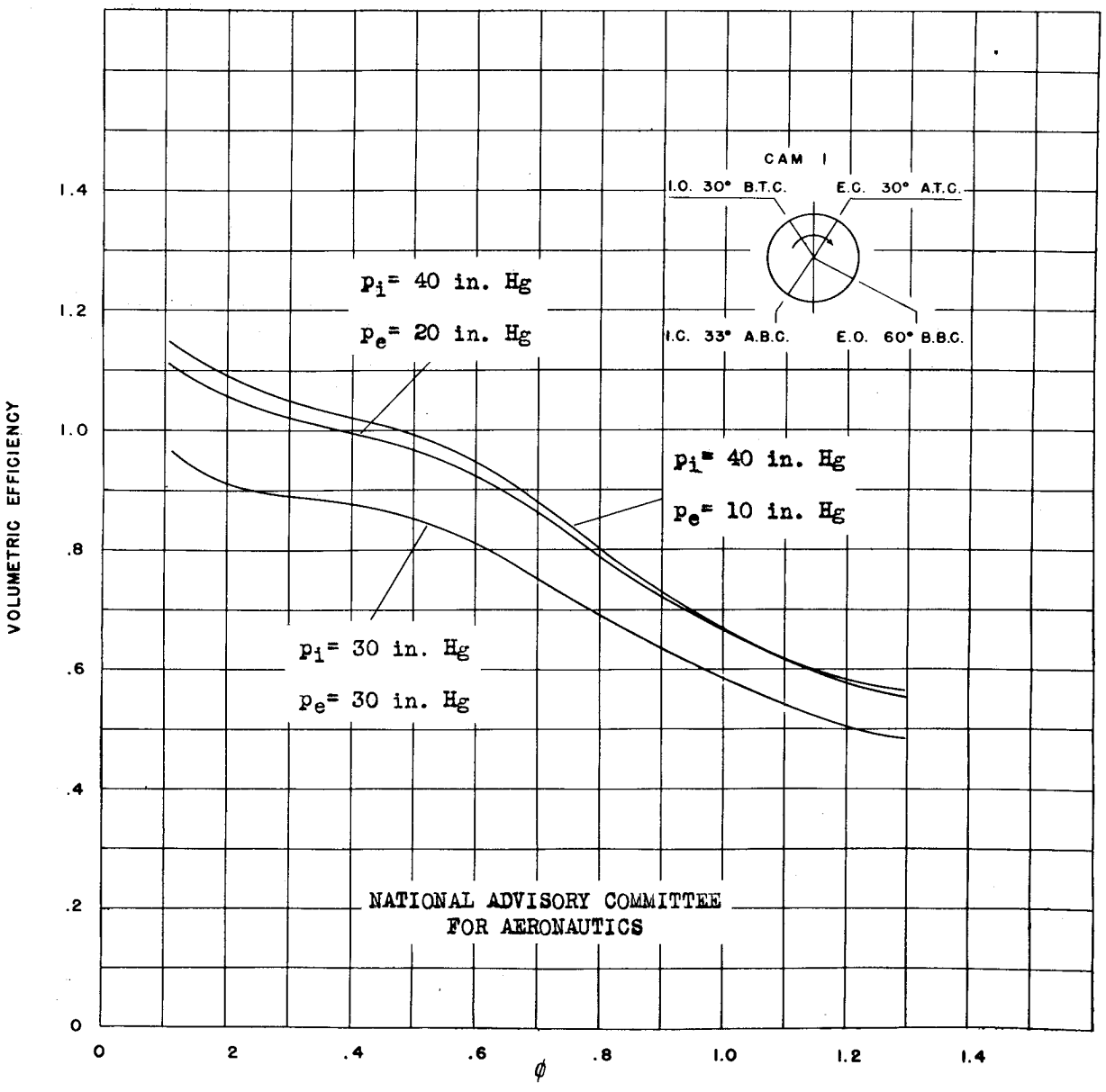


Figure 24.- The effect of inlet and exhaust pressures on volumetric efficiency. Curves are those appearing in figures 2, 3, and 4.

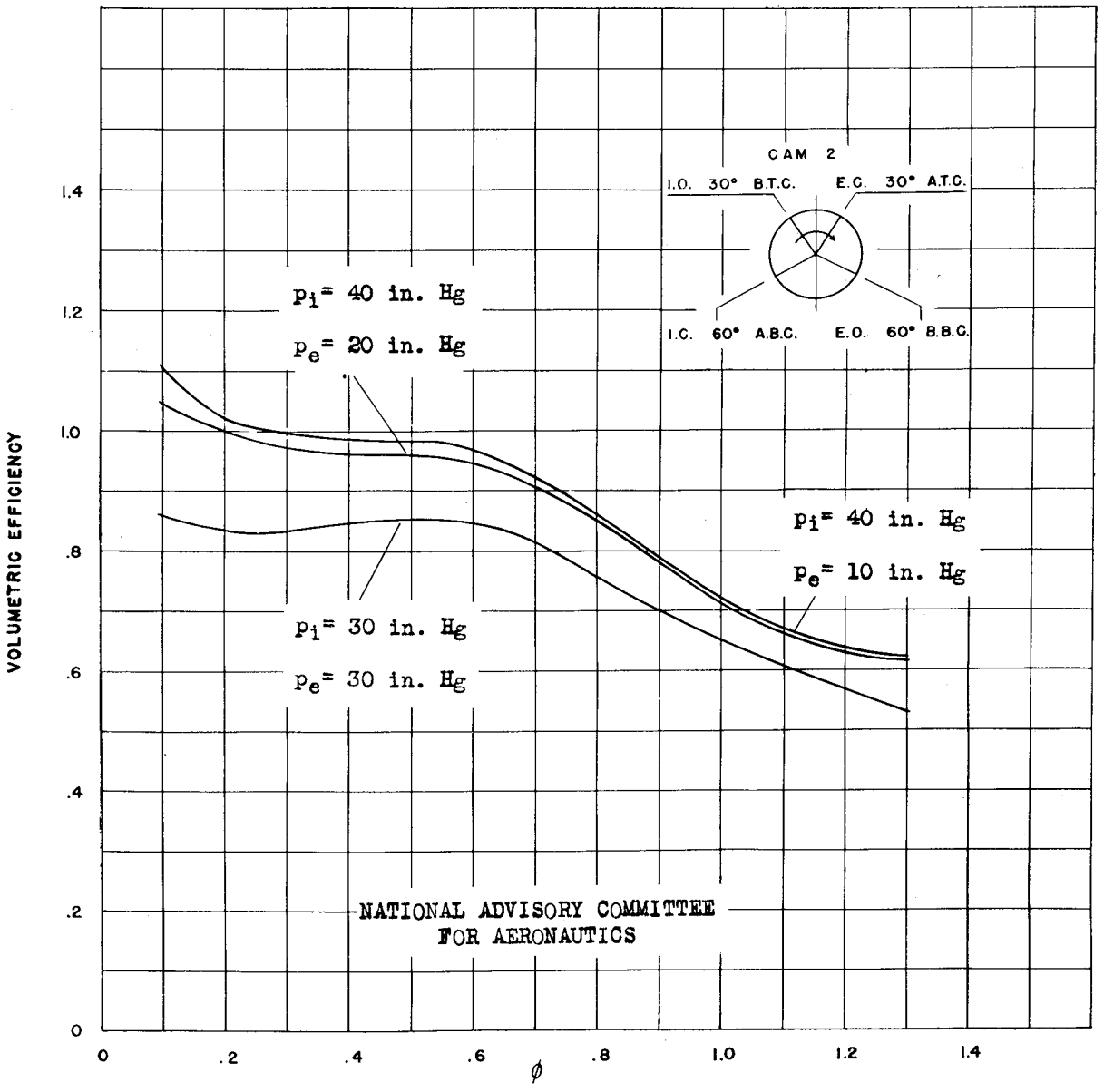


Figure 25.- The effect of inlet and exhaust pressures on volumetric efficiency. Curves are those appearing in figures 5, 6, and 7.

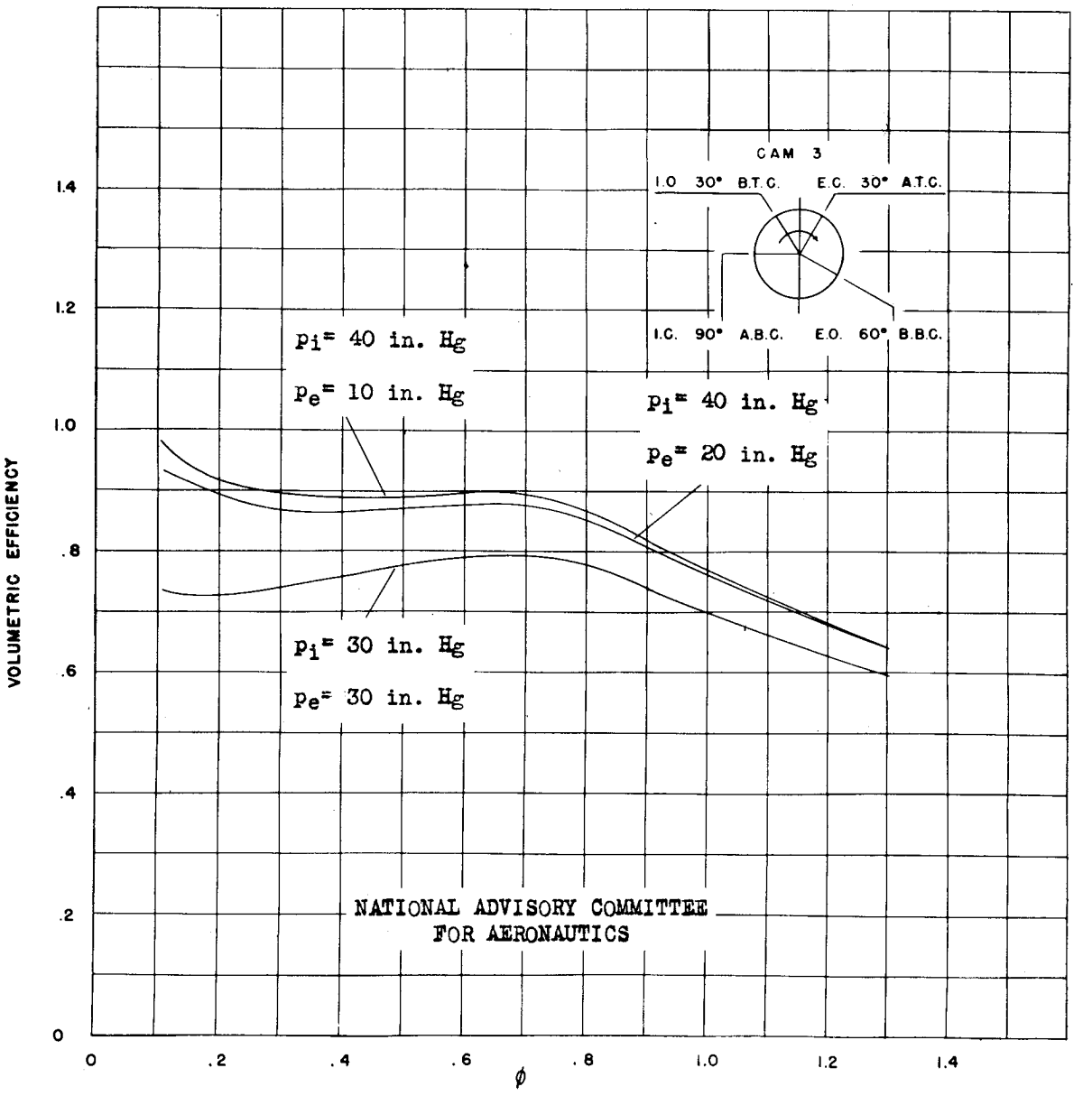


Figure 26.- The effect of inlet and exhaust pressures on volumetric efficiency. Curves are those appearing in figures 8, 9, and 10.

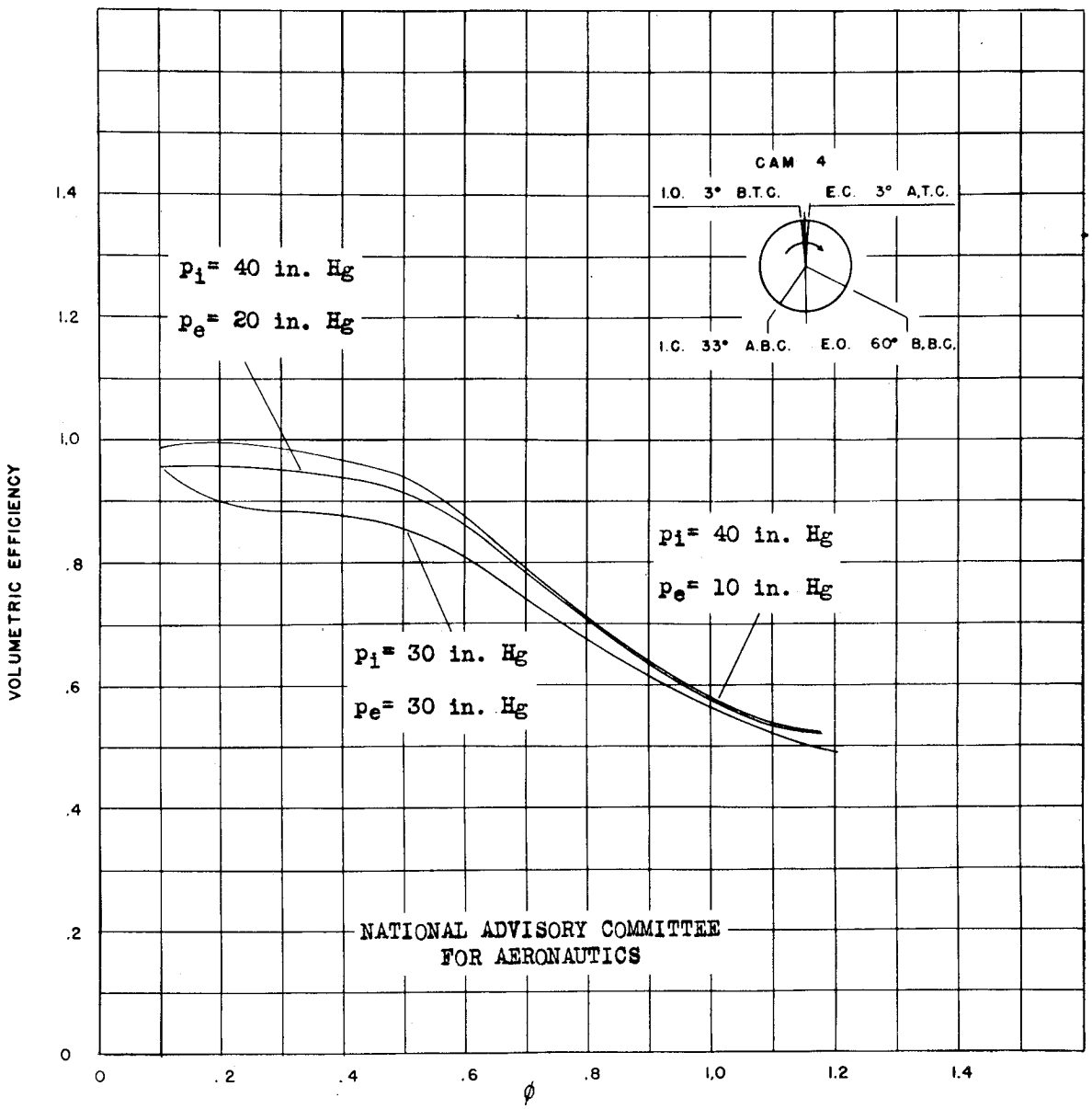


Figure 27.- The effect of inlet and exhaust pressures on volumetric efficiency. Curves are those appearing in figures 11, 12, and 13.

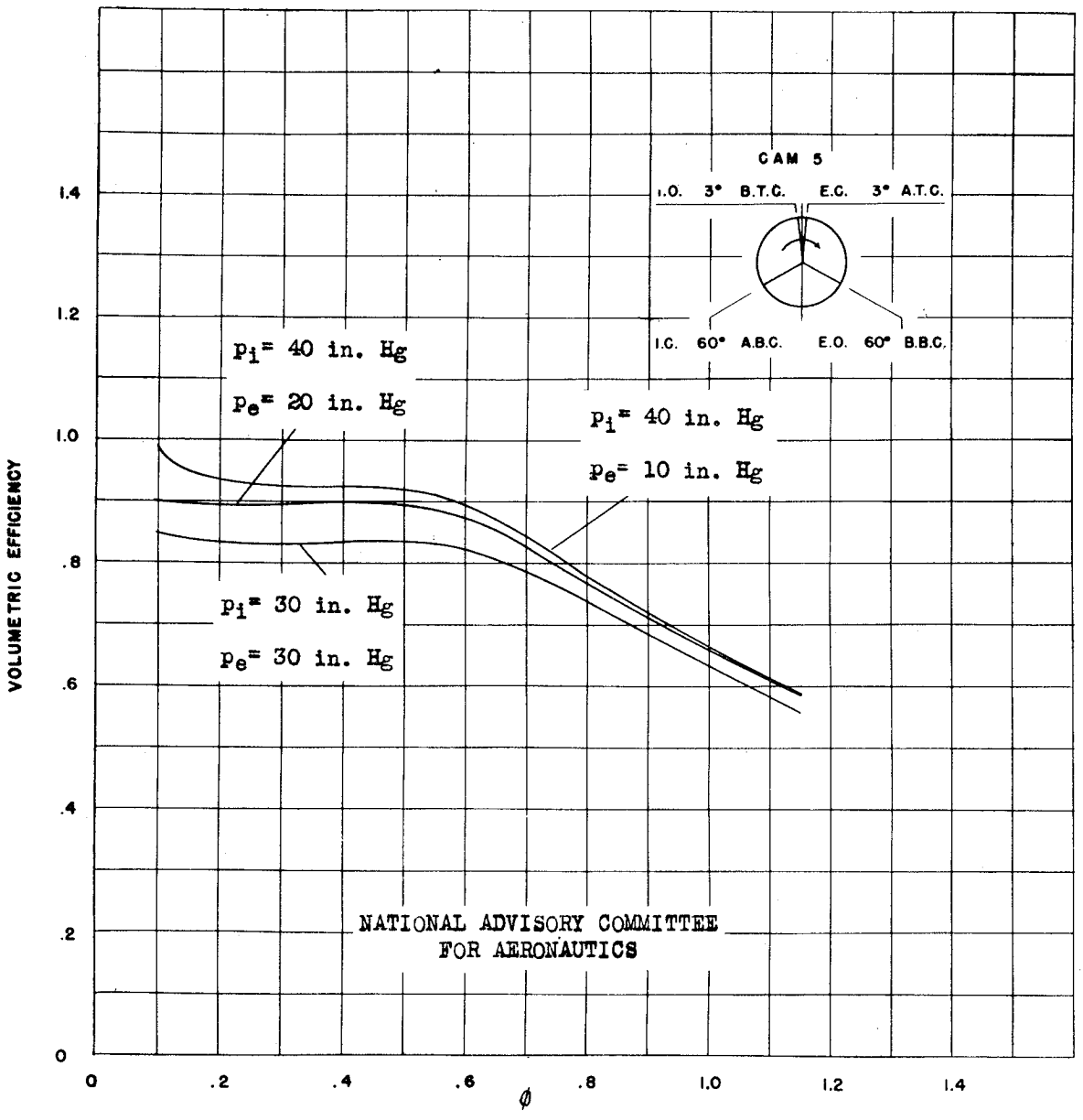


Figure 28.- The effect of inlet and exhaust pressures on volumetric efficiency. Curves are those appearing in figures 14, 15, and 16.

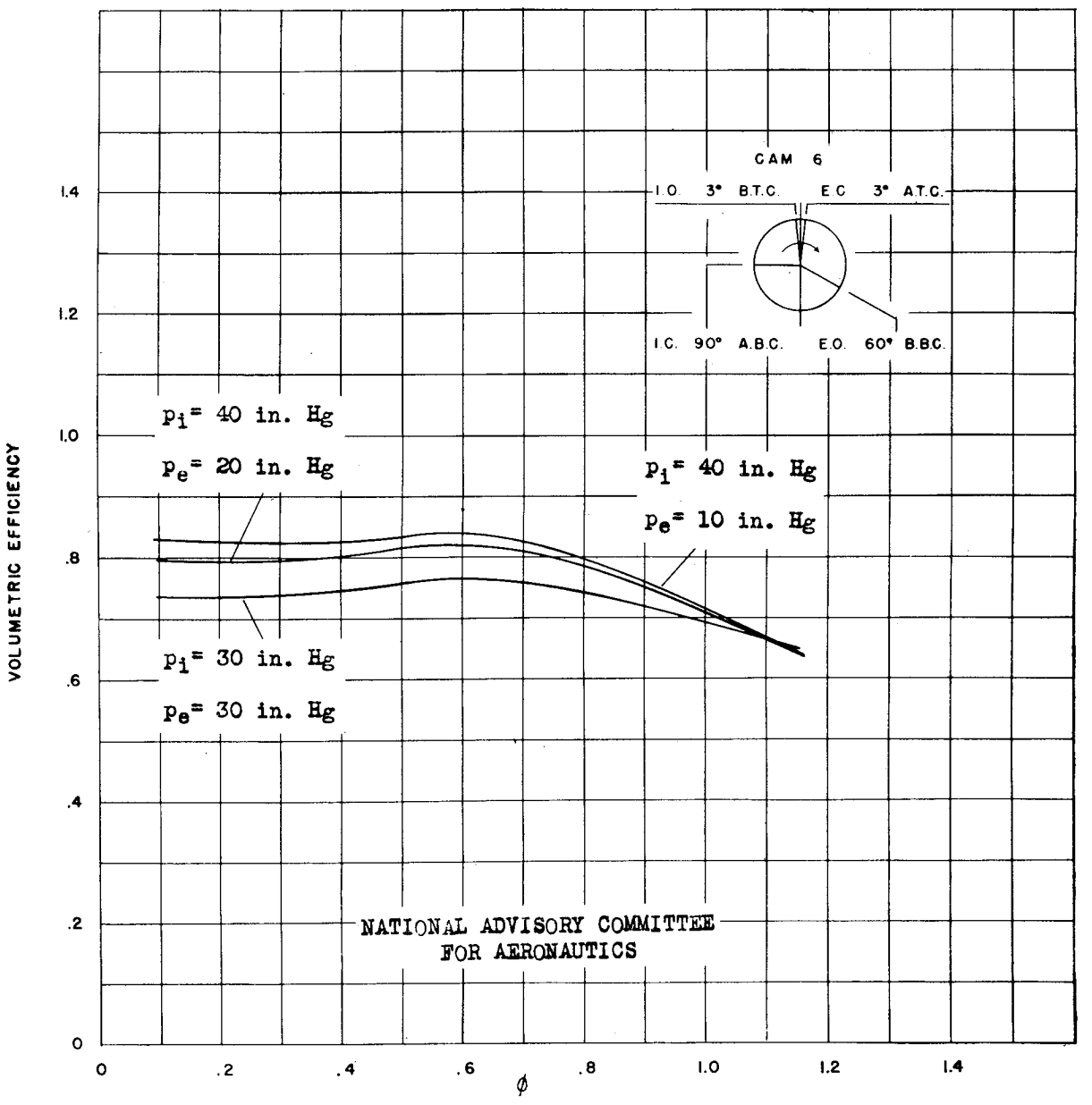


Figure 29.- The effect of inlet and exhaust pressures on volumetric efficiency. Curves are those appearing in figures 17, 18, and 19.

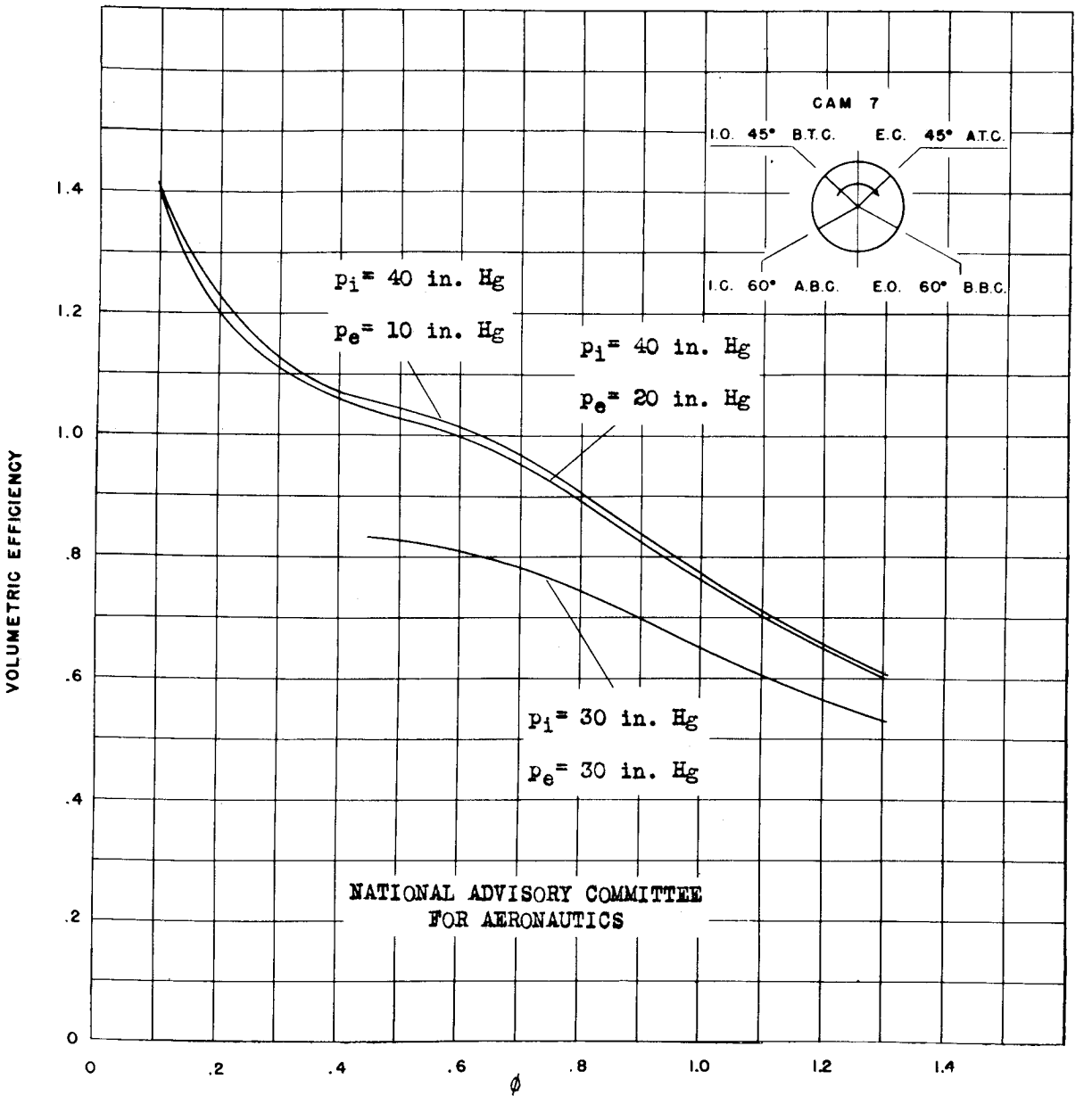


Figure 30.- The effect of inlet and exhaust pressures on volumetric efficiency. Curves are those appearing in figures 20, 21, and 22.

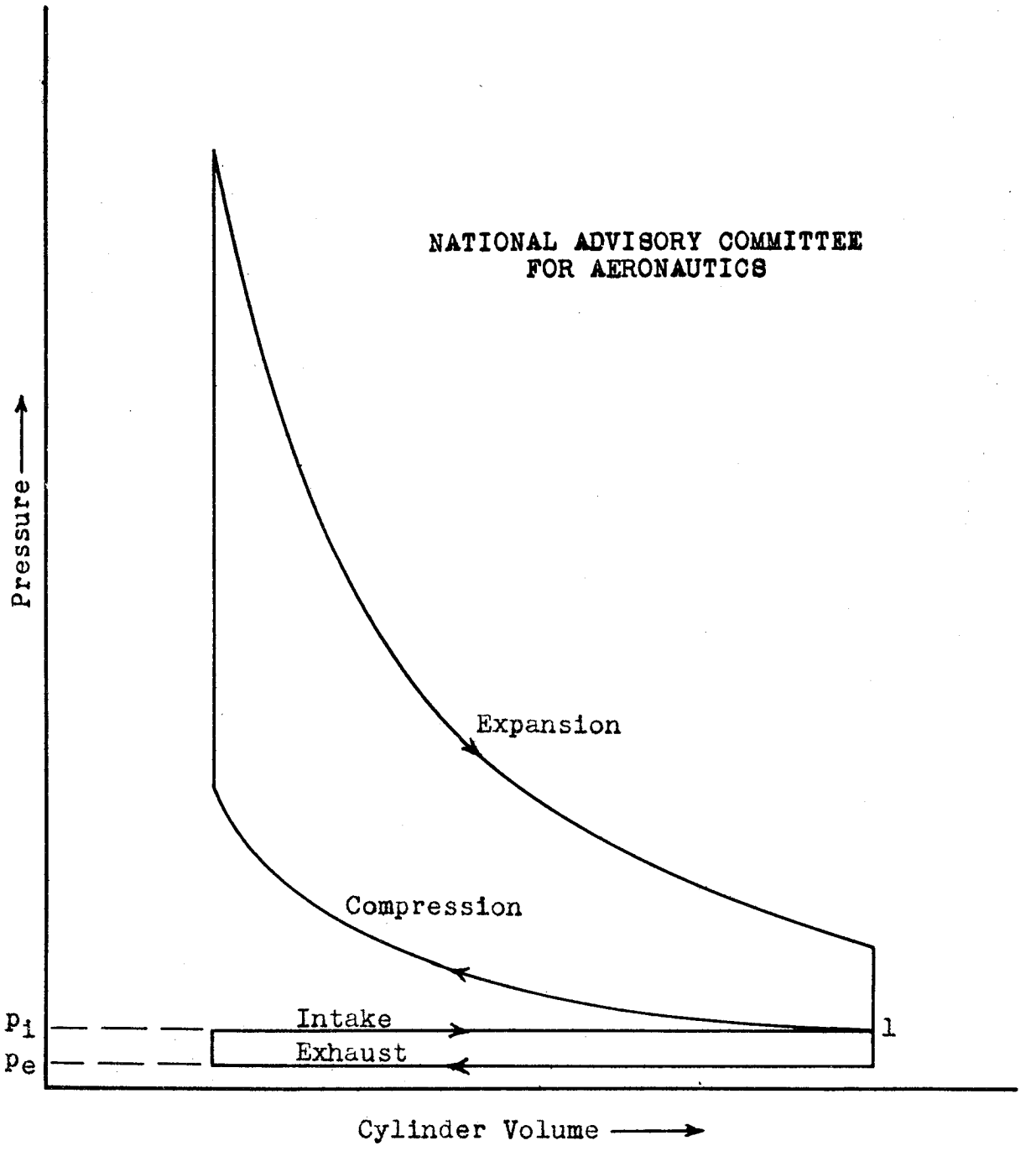


Figure 31.- "Square" pumping loop assumed for ideal air cycle.

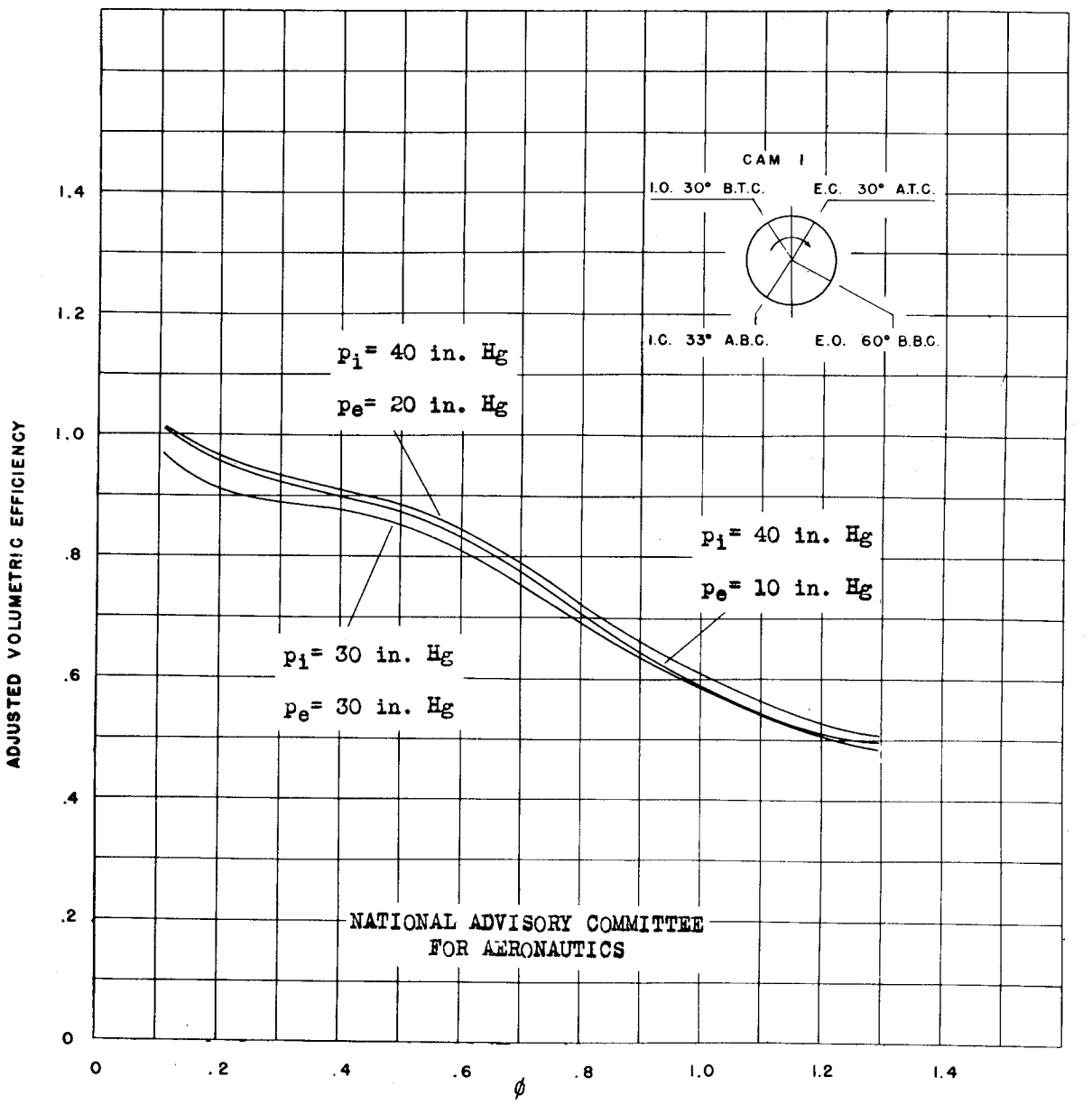


Figure 32.- Volumetric efficiency curves of figure 24 corrected for the effects of inlet and exhaust pressure.

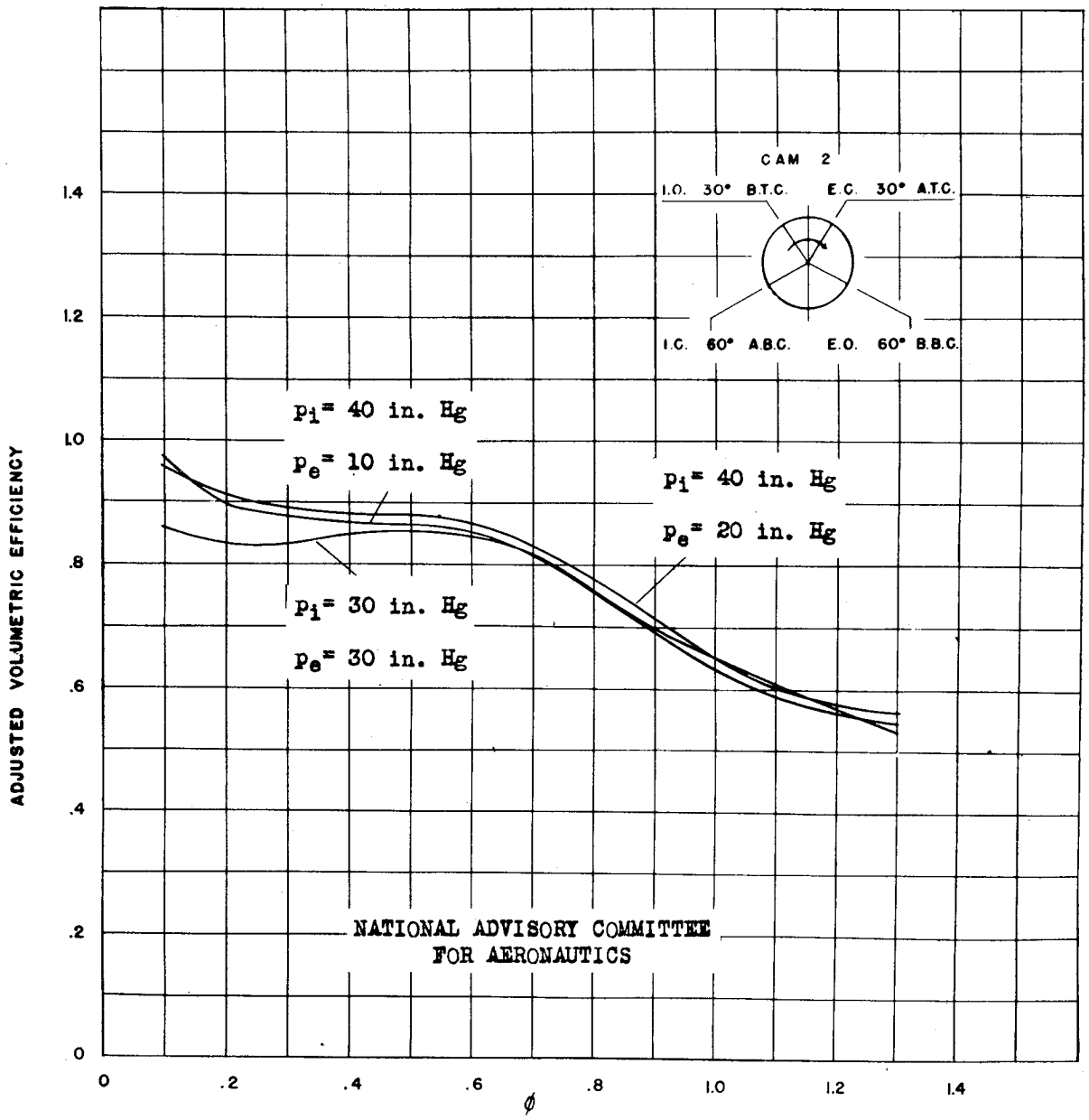


Figure 33.- Volumetric efficiency curves of figure 25 corrected for the effects of inlet and exhaust pressure.

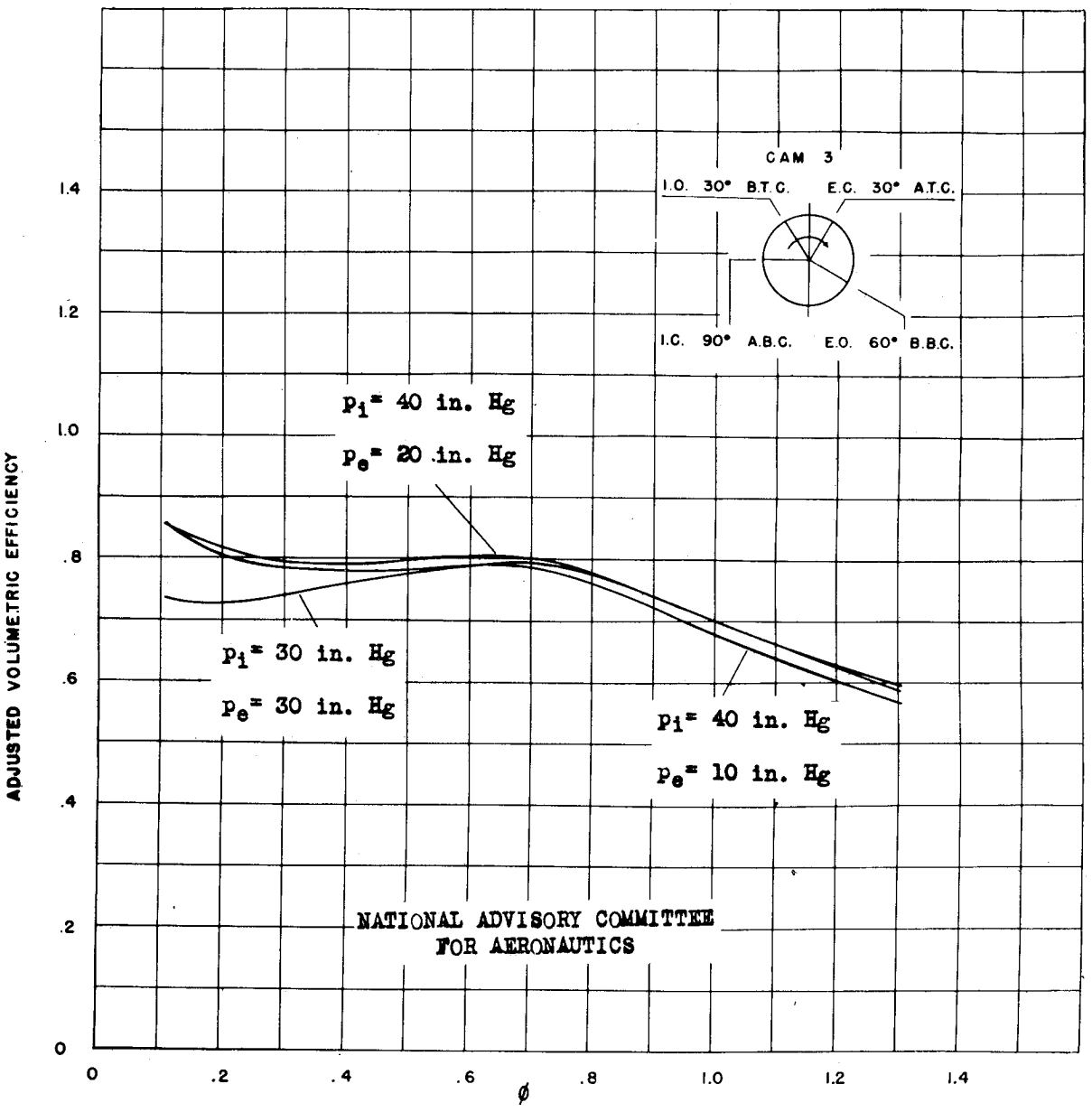


Figure 34.- Volumetric efficiency curves of figure 26 corrected for the effects of inlet and exhaust pressure.

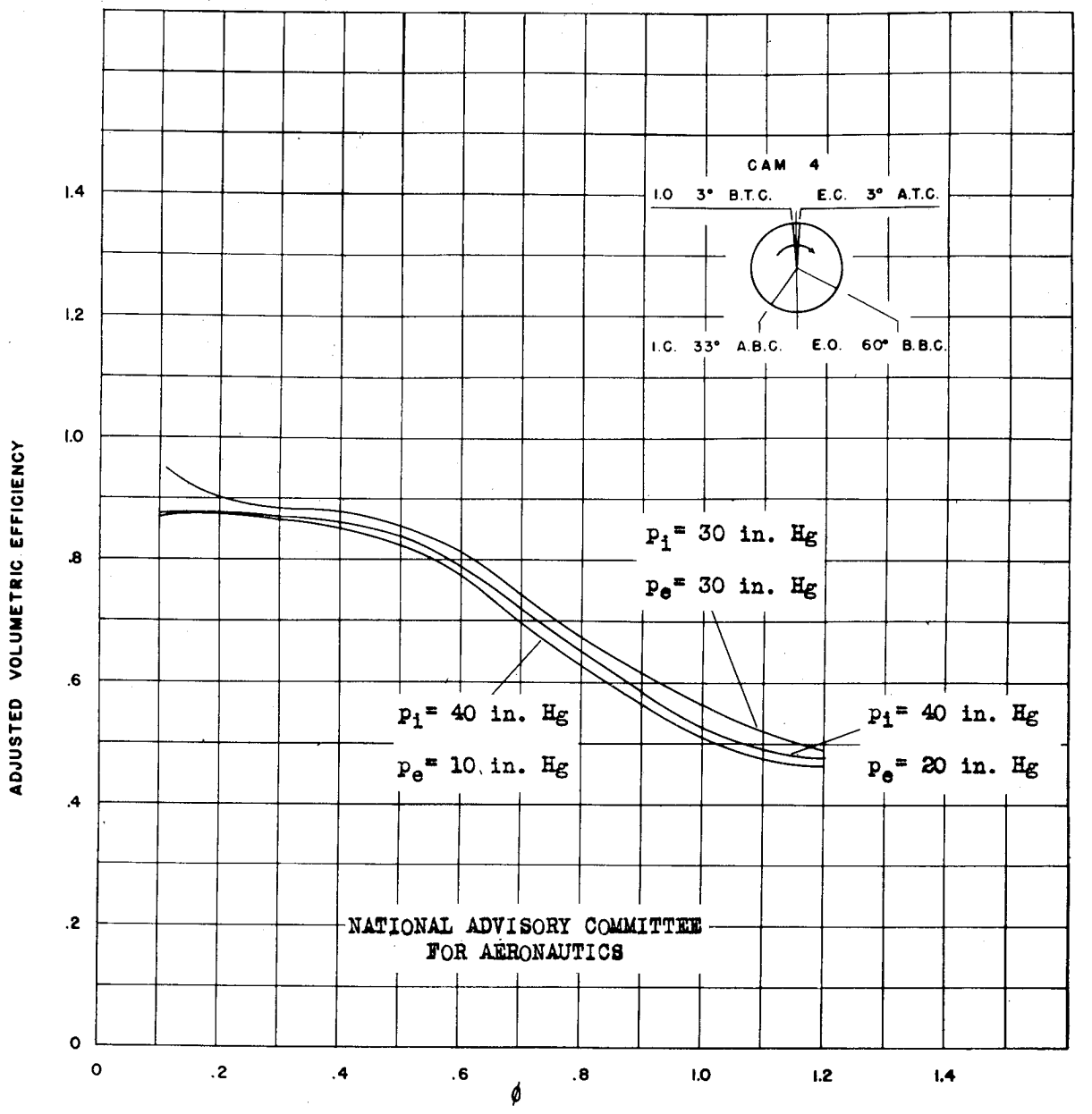


Figure 35.- Volumetric efficiency curves of figure 27 corrected for the effects of inlet and exhaust pressure.

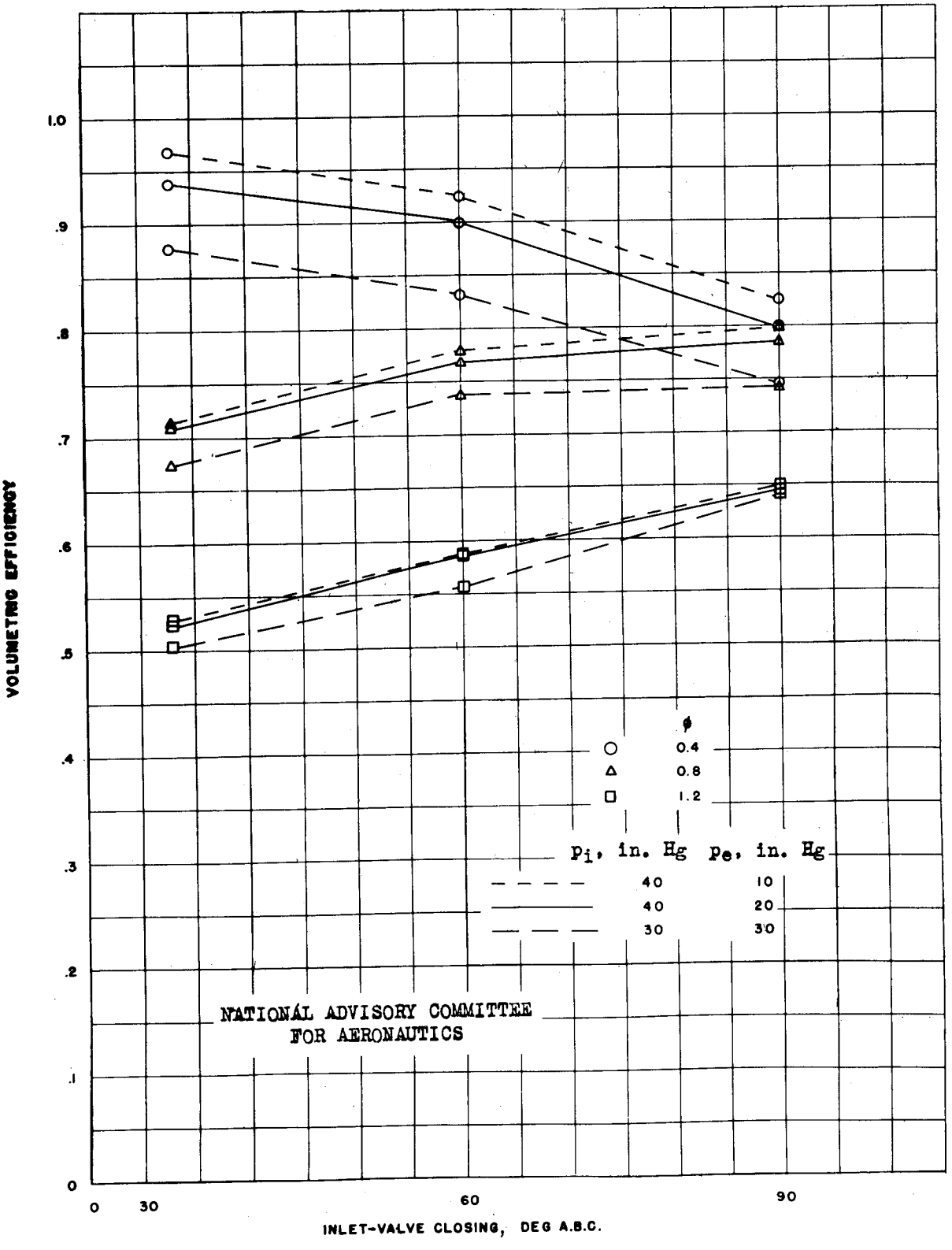


Figure 39.- The effect of inlet-valve closing angle on volumetric efficiency at several values of ϕ. Valves have 6° overlap. Exhaust opening, 60° B.B.C.

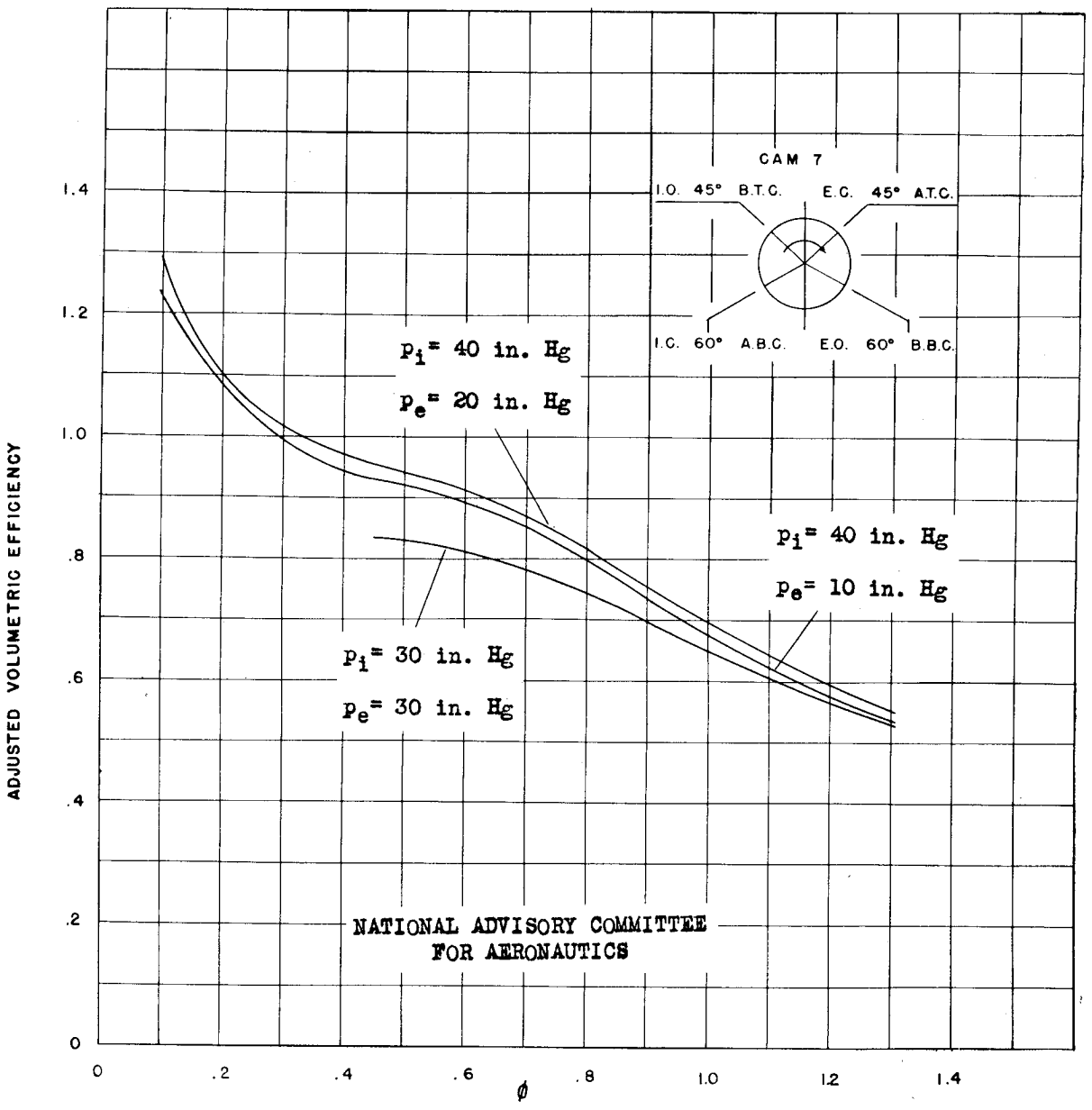


Figure 38.- Volumetric efficiency curves of figure 30 corrected for the effects of inlet and exhaust pressure.

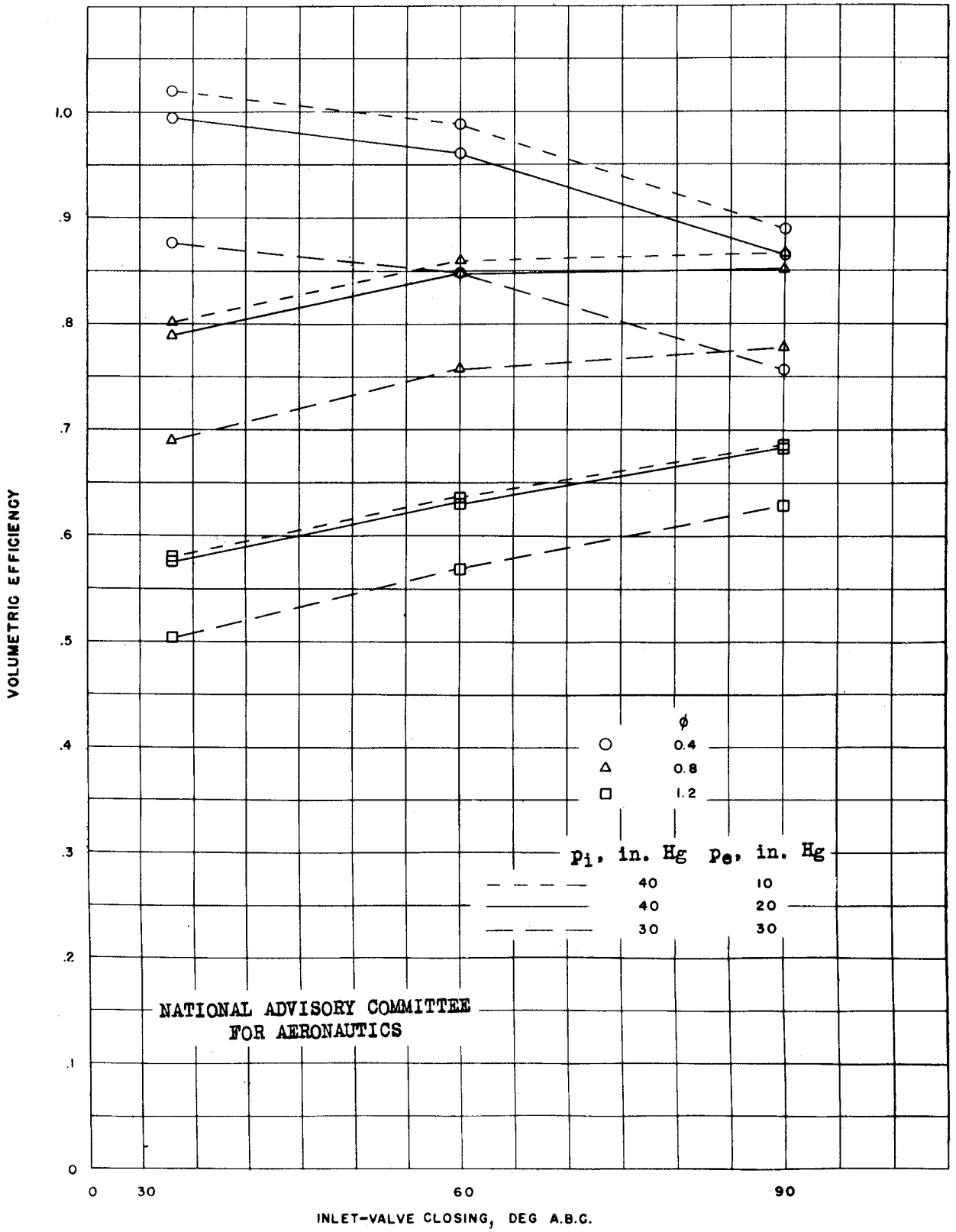


Figure 40.- The effect of inlet-valve closing angle on volumetric efficiency at several values of ϕ. Valves have 60° overlap. Exhaust opening, 60° B.B.C.

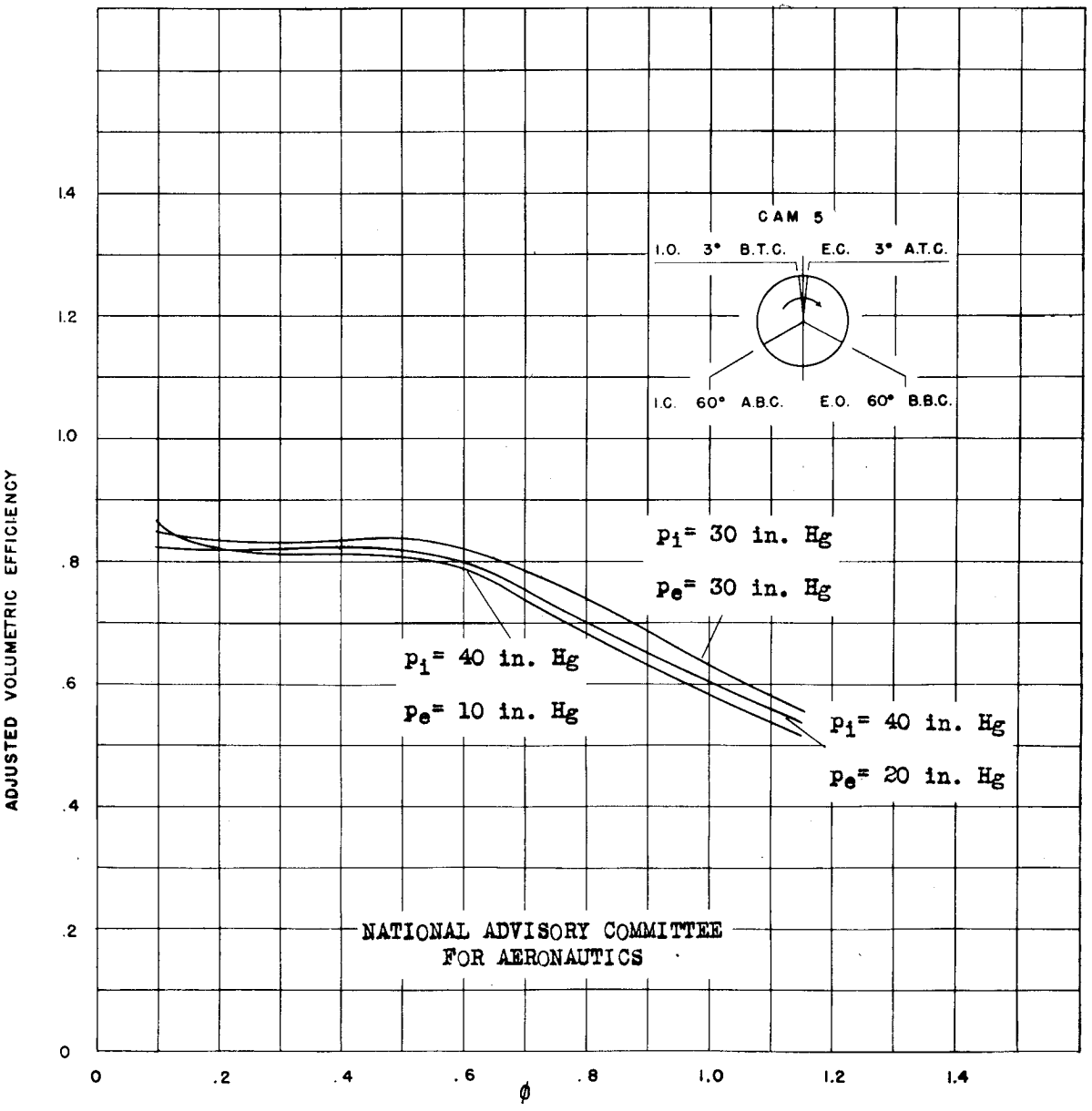


Figure 36.- Volumetric efficiency curves of figure 28 corrected for the effects of inlet and exhaust pressure.

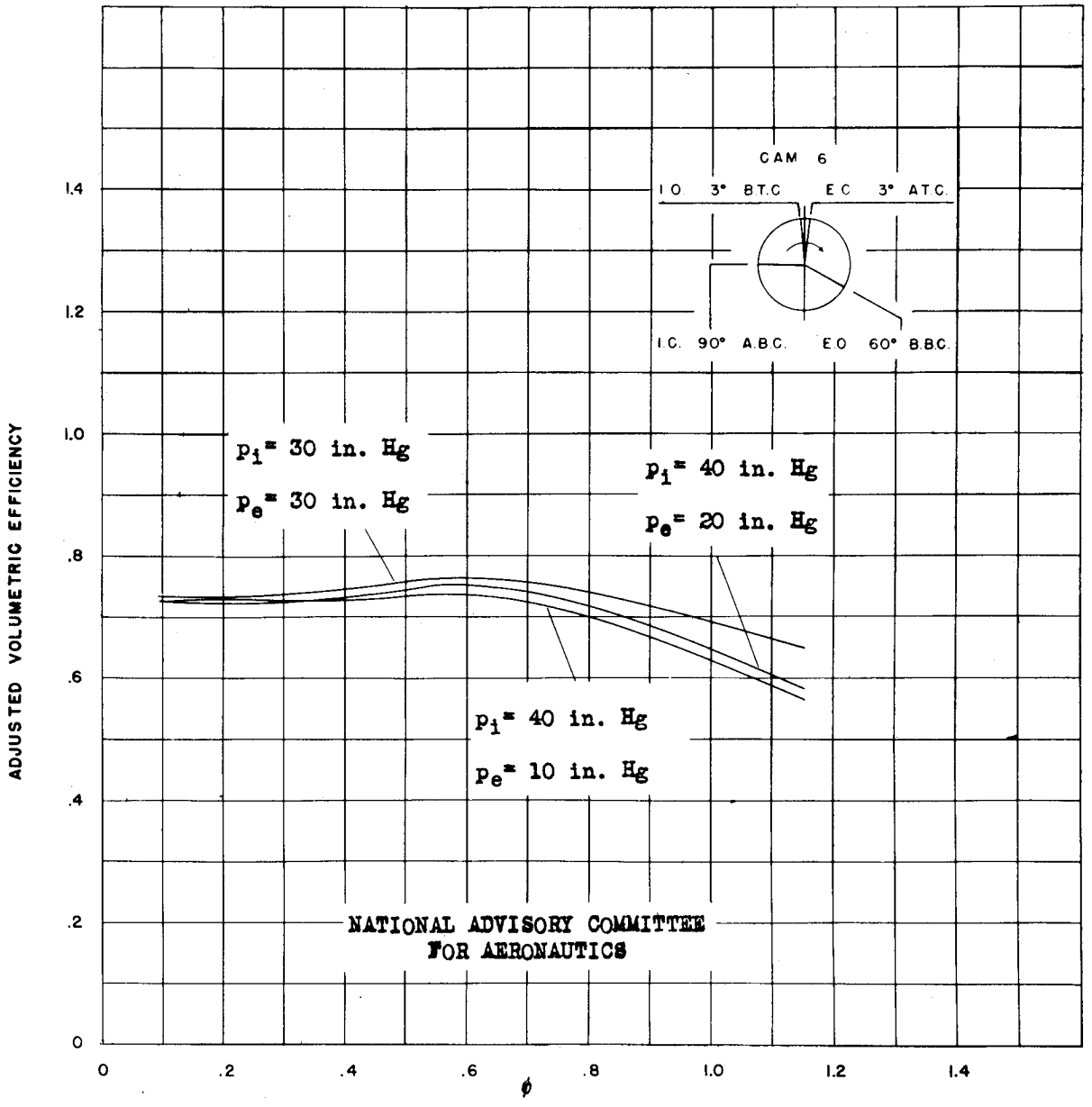


Figure 37.- Volumetric efficiency curves of figure 29 corrected for the effects of inlet and exhaust pressure.

NATIONAL ADVISORY COMMITTEE
FOR AERONAUTICS

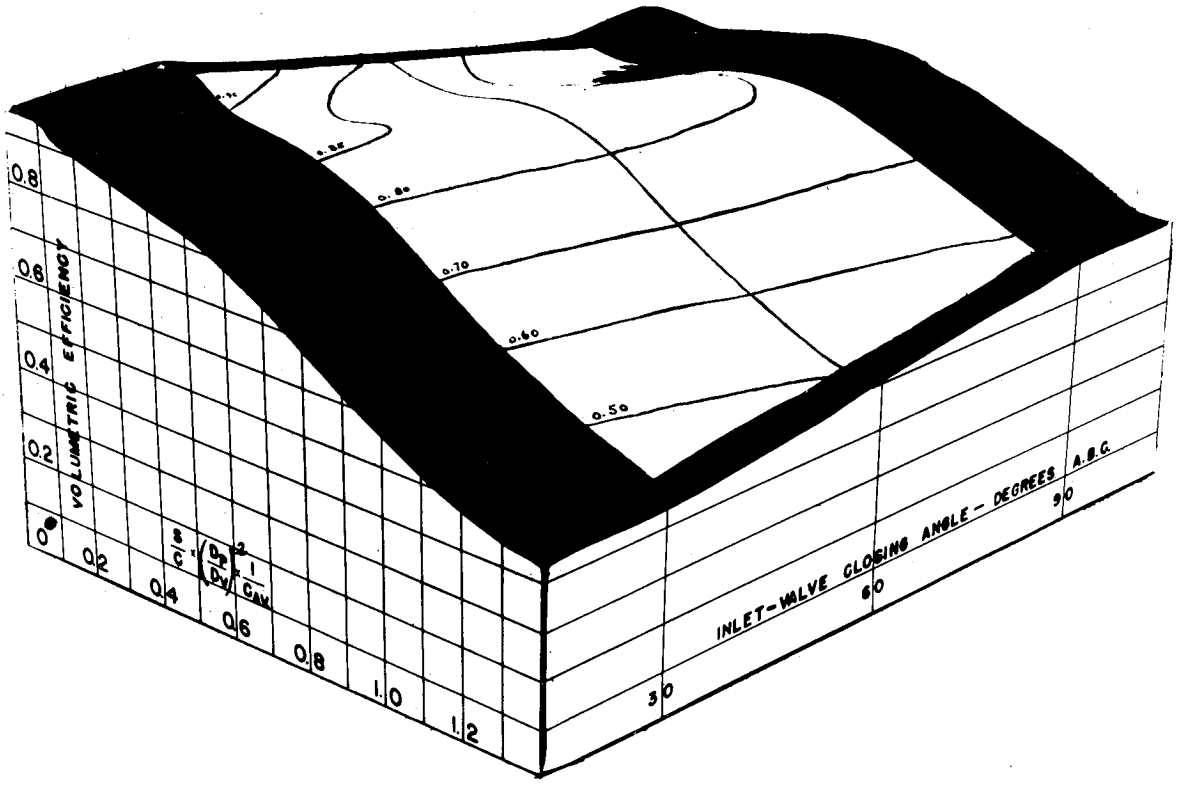


Figure 41.- Model showing effect of inlet-valve closing on volumetric efficiency at several values of Ø. $p_e = p_i = 30$ inches of mercury absolute. Valves have 60° overlap.

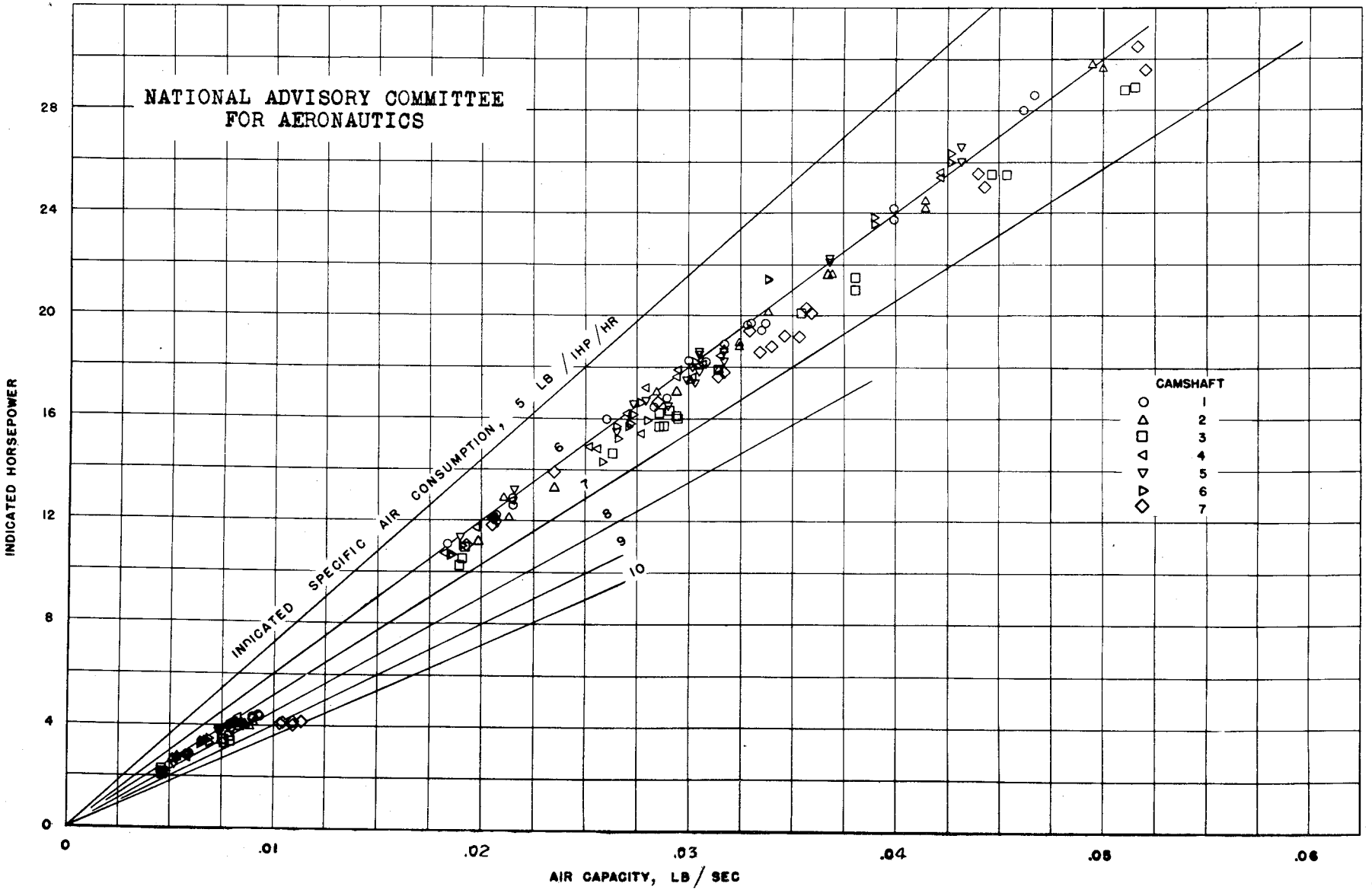


Figure 42.- Relationship between indicated horsepower and air flow.

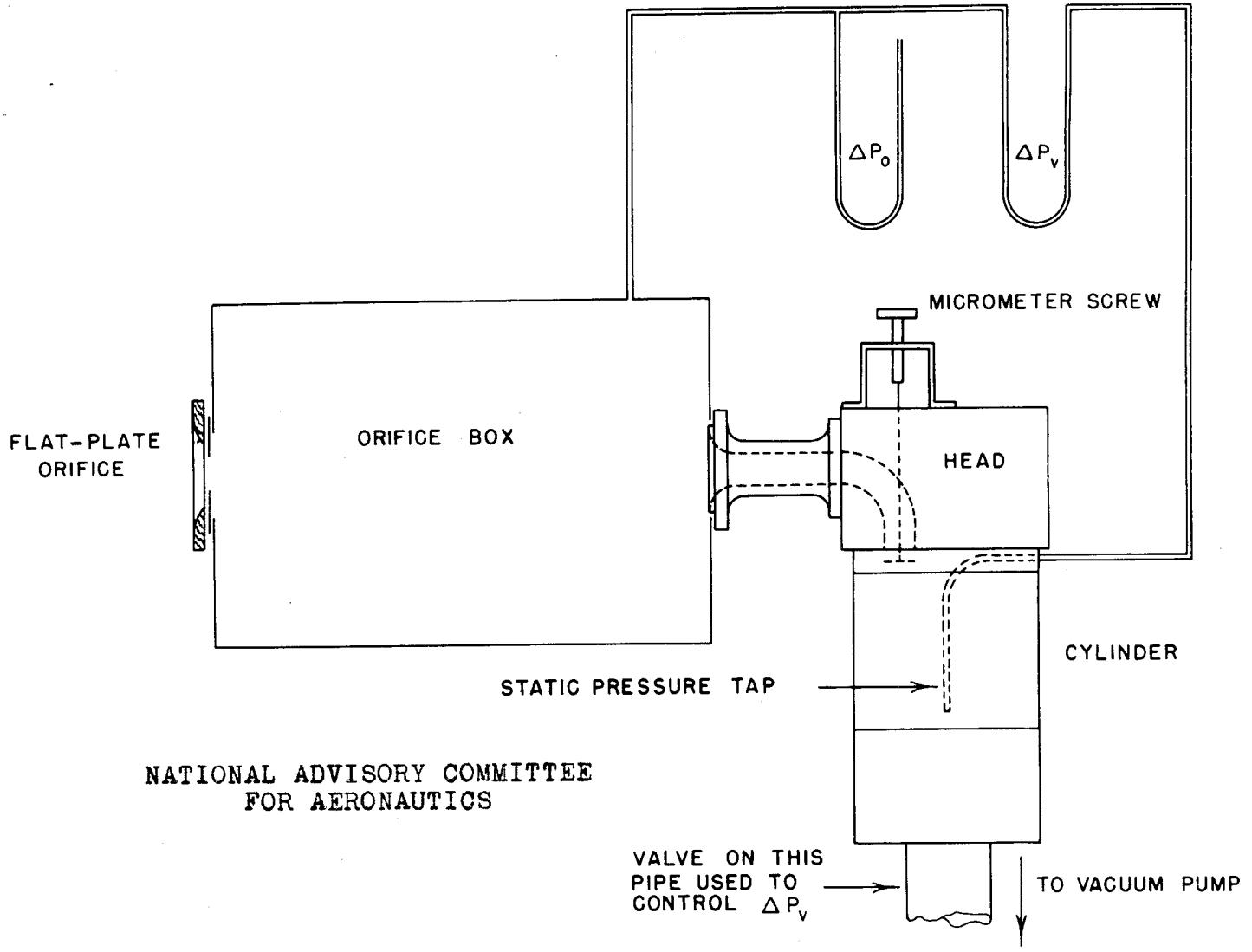


Figure 43.- Schematic layout of the steady-flow test apparatus.